US of the Inguinal Canal: Comprehensive Review of Pathologic Processes with CT and MR Imaging Correlation[1]

Margarita V. Revzin, MD, MS
Devrim Ersahin, MD
Gary M. Israel, MD
Jonathan D. Kirsch, MD
Mahan Mathur, MD
Jamal Bokhari, MD
Leslie M. Scoutt, MD

Abbreviations: IC = inguinal canal, PV = processus vaginalis

RadioGraphics 2016; 36:0000–0000

Published online 10.1148/rg.2016150181

Content Codes: CT GU MR US

[1]From the Department of Diagnostic Radiology, Yale University School of Medicine, 333 Cedar St, PO Box 208042, Room TE-2, New Haven, CT 06520. Recipient of a Certificate of Merit award for an education exhibit at the 2014 RSNA Annual Meeting. Received June 13, 2015; revision requested September 13 and received October 30; accepted February 3, 2016. For this journal-based SA-CME activity, the author L.M.S. has provided disclosures (see end of article); all other authors, the editor, and the reviewers have disclosed no relevant relationships. **Address correspondence to** M.V.R. (e-mail: *margarita.revzin@yale.edu*).

SA-CME LEARNING OBJECTIVES

After completing this journal-based SA-CME activity, participants will be able to:

- Describe embryologic development and relevant anatomic structures of the IC in male and female individuals and the relationships of these structures with inguinal pathologic processes.
- Determine proper US techniques for imaging the IC.
- Recognize US features of common and uncommon pathologic processes involving the IC.

See www.rsna.org/education/search/RG.

Ultrasonography (US) has a fundamental role in the initial examination of patients who present with symptoms indicating abnormalities of the inguinal canal (IC), an area known for its complex anatomy. A thorough understanding of the embryologic and imaging characteristics of the contents of the IC is essential for any general radiologist. Moreover, an awareness of the various pathologic conditions that can affect IC structures is crucial to preventing misdiagnoses and ensuring optimal patient care. Early detection of IC abnormalities can reduce the risk of morbidity and mortality and facilitate proper treatment. Abnormalities may be related to increased intra-abdominal pressure, which can result in development of direct inguinal hernias and varicoceles, or to congenital anomalies of the processus vaginalis, which can result in development of indirect hernias and hydroceles. US is also helpful in assessing postoperative complications of hernia repair, such as hematoma, seroma, abscess, and hernia recurrence. In addition, it is often the modality initially used to detect neoplasms arising from or invading the IC. US is an important tool in the examination of patients suspected of having undescended testes or posttraumatic testicular retraction and is essential for the examination of patients suspected of having torsion or infectious inflammatory conditions of the spermatic cord.

Online supplemental material is available for this article.

Introduction

Ultrasonography (US) has an important role in the initial assessment of pathologic processes of the inguinal canal (IC). It is critical for the radiologist to understand the embryologic development and detailed US-depicted anatomy of the IC to avoid misinterpretion of findings. Moreover, awareness of the US appearances of a broad spectrum of pathologic conditions affecting the IC will facilitate improved accuracy in interpretation of findings and help ensure proper treatment of patients.

In this article, we review the anatomy and embryologic development of the IC, optimal US scanning techniques, and imaging characteristics of both common and rare pathologic conditions of the IC. In addition, US findings are correlated with the findings of other imaging modalities.

TEACHING POINTS

- An indirect inguinal hernia occurs when abdominal contents protrude through the deep inguinal ring and course anteromedially to the spermatic cord in the IC. The hernia contents emerge by way of the superficial ring and often descend into the scrotum or labia majora.
- The deep inguinal ring is the neck of an indirect inguinal hernia and is located lateral to the origin of the inferior epigastric vessels. The neck of a direct inguinal hernia lies medial to the inferior epigastric vessels within the Hesselbach triangle.
- There are two major types of IC hydrocele—communicating and noncommunicating. With a communicating hydrocele, there is communication of fluid between the peritoneal cavity and scrotum due to complete patency of the PV.
- Isolated right-sided varicoceles are seen in only 6% of patients, and if they are detected, the retroperitoneum and abdomen should be evaluated for any pathologic process—most commonly a neoplasm.
- At imaging, nonpalpable testes can be localized by using the tracking technique. With this technique, the spermatic cord is used as a guide to find the testes. Initially, one can identify the spermatic cord in the IC at the deep inguinal ring by scanning in a sagittal oblique plane on the short axis relative to the IC. Once found, the cord can be "tracked" inferiorly in an attempt to locate the testis along the path of testicular descent.

Embryologic Development of the IC

The ICs develop in both male and female individuals. The processus vaginalis (PV), an evagination of the parietal peritoneum, and the gubernaculum, a fibromascular ligament, have major roles in the development of the IC.

At 7 weeks gestation, the gubernaculum has developed. In male embryos, the cranial end of the gubernaculum is attached to the inferior pole of the testes and the caudal end is attached to the labioscrotal fold. The gubernaculum assists in the descent of the testes from their intra-abdominal position into the developing scrotum (Fig 1) (1–3).

In female embryos, the cranial end of the gubernaculum is attached to the ovaries and the caudal end is attached to the internal surface of the labioscrotal fold. Midpoint attachment of the gubernaculum to the uterus prevents the ovaries from descending into the ICs. The cranial portion of the gubernaculum later becomes the ovarian ligament, and the caudal portion becomes the round ligament of the uterus. The round ligaments pass through the ICs and terminate in the labia majora (1).

The PV, also known as the diverticulum of the parietal peritoneum, develops during the 2nd and 3rd months of gestation and lies ventral to the gubernaculum (Fig 1). The PV herniates through the abdominal wall along a path formed by the gubernaculum, and in male fetuses, it passes into the developing scrotum. Extensions of the layers of the abdominal wall accompany the PV and form the walls of the IC. In male fetuses, these layers also form the coverings of the spermatic cord and testes (Fig 2). The opening of the transversalis fascia produced by the PV becomes the deep inguinal ring, and the triangular opening in the external oblique aponeurosis from which the PV emerges becomes the superficial inguinal ring. The superior portion of the PV usually closes at or just before birth, and obliteration proceeds gradually in a downward direction (Fig 2). In the male fetus, the scrotal portion of the PV remains patent, forming the tunica vaginalis of the testicle; in the female fetus, it degenerates before birth. A persistently patent PV will allow communication between the tunica vaginalis and the peritoneal cavity. In female fetuses, a persistently patent PV is called the canal of Nuck (4).

Normal Anatomy of the IC

The IC is an oblique inferomedially directed 4-cm passage that is lined by the aponeuroses of three abdominal wall muscle groups (Fig 3). These abdominal wall muscles form the anterior and posterior walls, roof, and floor of the IC (Fig 4) (5,6). The IC lies parallel and cranial to the medial half of the inguinal ligament. The deep inguinal ring marks the entrance to the IC and is produced by an outpouching of the transversalis fascia. The transversalis fascia continues into the canal, forming the innermost covering (ie, internal fascia) of the IC. The superficial inguinal ring, a slit-like opening in the external oblique aponeurosis, represents the exit site from the IC through which the spermatic cord (in male persons) and round ligament (in female persons) emerge and lies superolateral to the pubic tubercle. The IC contains blood, lymph vessels, and the ilioinguinal nerve in both sexes, in addition to the spermatic cord in male individuals and the round ligament in female individuals (Fig 5) (4).

The inferior epigastric vessels represent one of the major anatomic landmarks that help localize the deep inguinal ring (7). They arise from the external iliac artery and vein immediately above the inguinal ligament, course in an upward oblique direction along the medial margin of the internal inguinal ring, and anastomose with the superior epigastric vessels at the level of the umbilicus. The deep inguinal ring is located just lateral and slightly cranial to the origin of the inferior epigastric artery. The Hesselbach triangle represents an anatomic area defined medially by the lateral border of the rectus abdominis muscle, superolaterally by the inferior epigastric vessels, and inferiorly by the inguinal ligament (8).

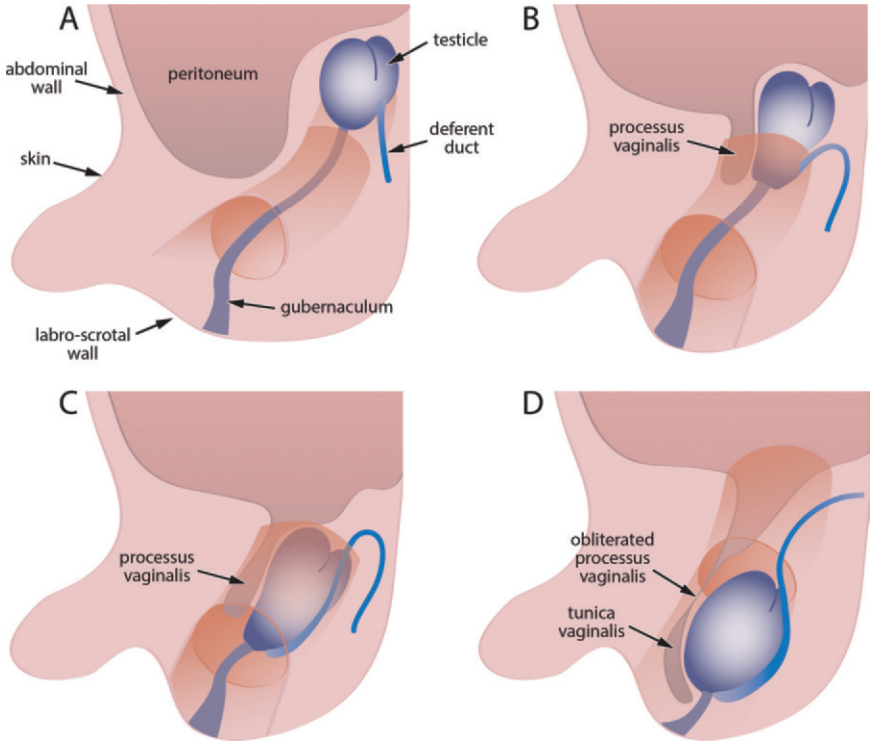

Figure 1. Diagram of the embryologic development of the IC. *A,* At 7 weeks gestation, the gubernaculum passes through the developing anterior abdominal wall at the site of the future IC. The gubernaculum is attached to the lower pole of the extraperitoneally located testes. *B,* At 7–12 weeks gestation, the gubernaculum shortens and pulls the testes to the level of the deep inguinal ring. The PV invaginates through the anterior abdominal wall along a path formed by the gubernaculum. Extensions of the layers of the abdominal wall accompany the PV and form the walls of the IC. *C,* At 26–28 weeks gestation, with androgenic stimulation and increased intra-abdominal pressure, the PV and testes begin to pass through the IC. It takes 2–3 days for the testes to reach the scrotum. *D,* At 32–40 weeks gestation, the IC is formed, and there is downward gradual obliteration of the PV. The scrotal portion of the PV remains patent, forming the tunica vaginalis.

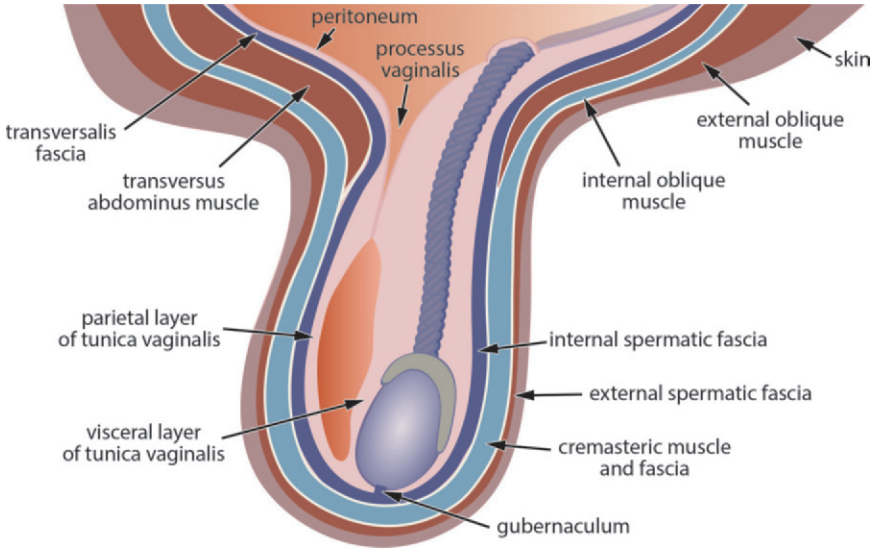

Figure 2. Diagram of the IC and scrotum shows obliteration of the superior portion of the PV. During development, extensions of all layers of the abdominal wall accompany the PV and contribute to the formation of the walls of the IC and scrotum. The PV is anterior (ventral) to the spermatic cord and developing testis. The parietal and visceral layers of the tunica vaginalis are formed from the patent scrotal portion of the PV. The testes and spermatic cord remain retroperitoneal throughout their descent.

Anatomy of the Spermatic Cord

The contents of the spermatic cord include the ductus (vas) deferens, a 45-cm-long tube that transports sperm from the epididymis to the ejaculatory duct; the testicular, cremasteric, and deferential arteries and veins (pampiniform plexus); the genital branch of the genitofemoral nerve, which supplies the cremaster muscle; the lymphatic vessels; and connective tissue. The pampiniform plexus is a network of small veins that drain into the right or left testicular veins. Sympathetic nerve fibers are present on arteries and the ductus deferens. Fascial layers from the three abdominal wall muscle aponeuroses cover the spermatic cord (Fig 5) (6).

Physiologic Features of the IC

In adults, the deep and superficial rings of the IC do not overlap because of the oblique path of the IC. In the healthy individual, increased intra-abdominal pressure will force the posterior wall of the IC against the anterior wall and thus strengthen this wall and decrease the likelihood of herniation. Contraction of the external oblique muscle also brings together the anterior and posterior IC walls and serves to maintain the integrity of the IC. In addition, contraction of the internal oblique and transverse abdominis muscles causes the canal to constrict by causing

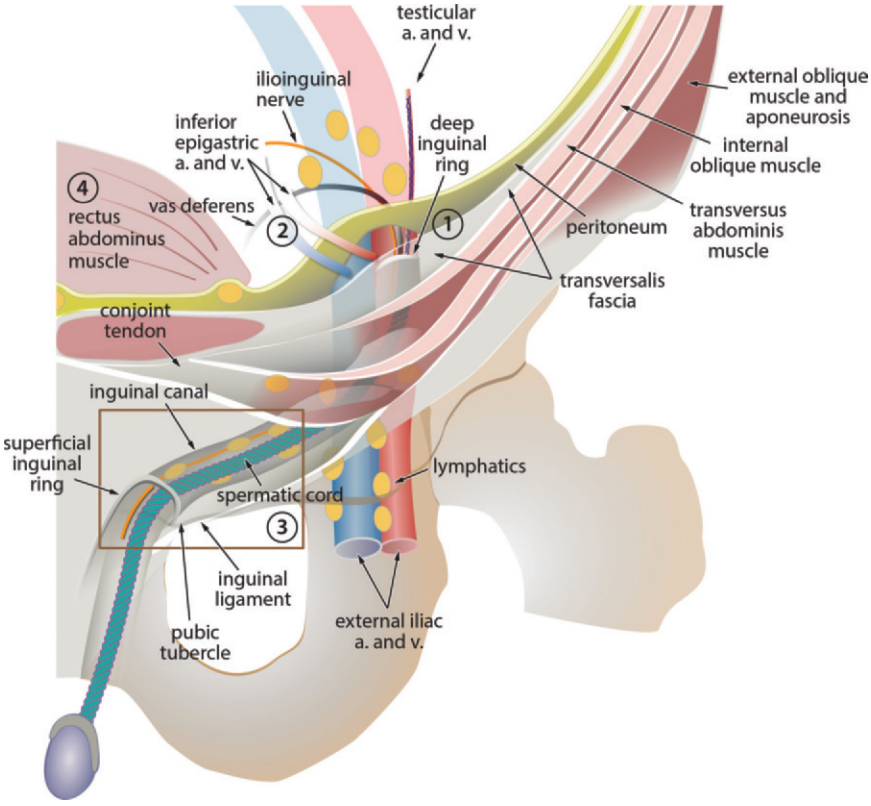

Figure 3. Diagram of the IC and its contents. The deep inguinal ring is formed by the transversalis fascia, and the IC is lined by the same layers that line the abdominal wall. The external superficial ring is a triangular opening in the oblique aponeurosis. The inferior epigastric artery *(a.)* and vein (*v.)* originate from the external iliac artery and vein and lie medial to the internal inguinal ring. The locations of the abdominal wall hernias in relation to the IC are as follows: The indirect inguinal hernias lie lateral to the inferior epigastric arteries *(1);* the direct inguinal hernias lie medial and inferior to the inferior epigastric vessels *(2);* the femoral hernias lie inferior and medial to the femoral vessels *(3);* and the spigelian hernias lie lateral to the rectus abdominus muscle *(4).*

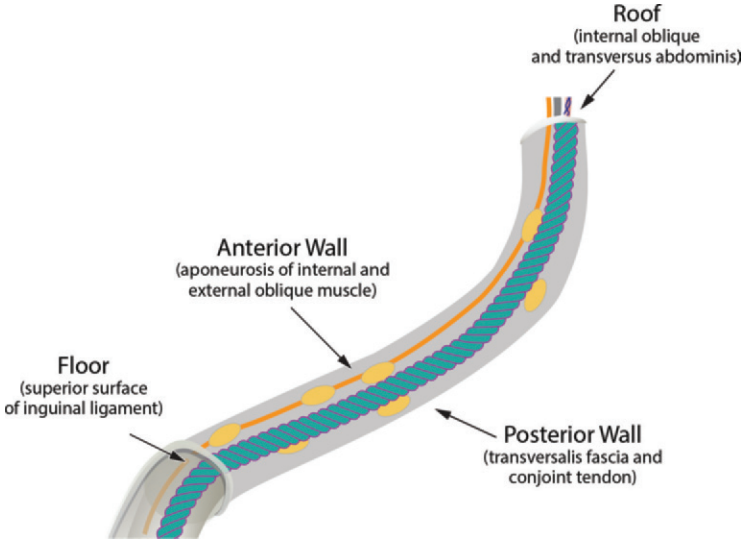

Figure 4. Diagram of the walls of the IC. The anterior wall is formed by the aponeuroses of the external and internal oblique muscles. The posterior wall is formed by the transversalis fascia and conjoint tendon, a medial juncture of the internal oblique and transversalis fasciae at the pectineal line. The roof, or superior wall, is formed by the aponeuroses of the internal oblique and transversus abdominis muscles. The floor, or inferior wall, of the IC is formed by the inguinal ligament, a folded-up border of the external oblique aponeurosis.

the roof to descend (Fig 4). If intra-abdominal pressure associated with pathologic processes is greater than the resistant effect of this mechanism, a hernia may develop.

US Technique for Evaluation of the IC

Because US can facilitate real-time imaging during dynamic patient maneuvers, it offers substantial advantages in evaluation of the IC compared with other cross-sectional imaging modalities such as computed tomography (CT) and magnetic resonance (MR) imaging, and provocative maneuvers may aid in visualization of pathologic processes of the IC—such as reducible hernias and varicoceles—that can be missed with static imaging alone. However, in some instances, CT and MR imaging may reveal important additional information, especially if a large field of view is required or an abdominal extension must be assessed.

US evaluation of the IC should be optimized on the basis of the clinical question being addressed. For most applications, a high-frequency (ie, 10–12-MHz) linear transducer is used. Low-

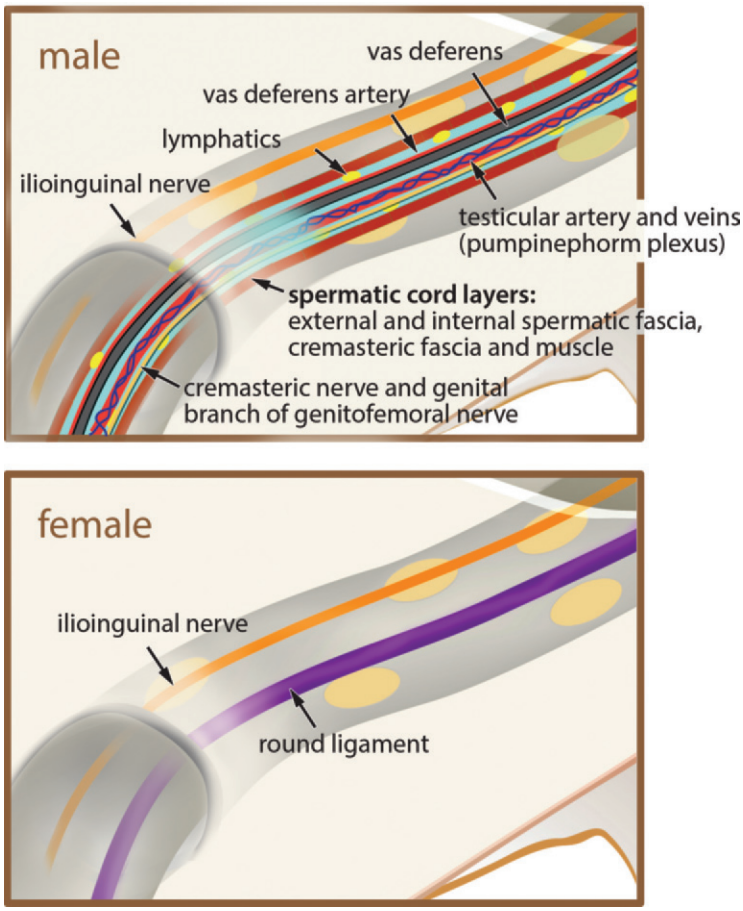

Figure 5. Diagrams of the contents of the IC in male and female individuals. In male individuals, the IC contains the ilioinguinal nerve and spermatic cord. The spermatic cord contains the genital branch of the genitofemoral nerve (from the lumbar plexus); vas deferens and vas deferens artery (a branch of the inferior vesicle artery); testicular artery, which originates from the infrarenal aorta; testicular veins (pumpiniform plexus), with the left testicular vein draining into the left renal vein and the right testicular vein draining directly into the inferior vena cava; cremasteric artery (a branch of the inferior epigastric artery); lymphatic vessels; and connective tissue. The external and internal spermatic fasciae and the cremasteric fascia and muscle cover the spermatic cord. In female individuals, the IC contains the ilioinguinal nerve, round ligament, and lymphatic vessels.

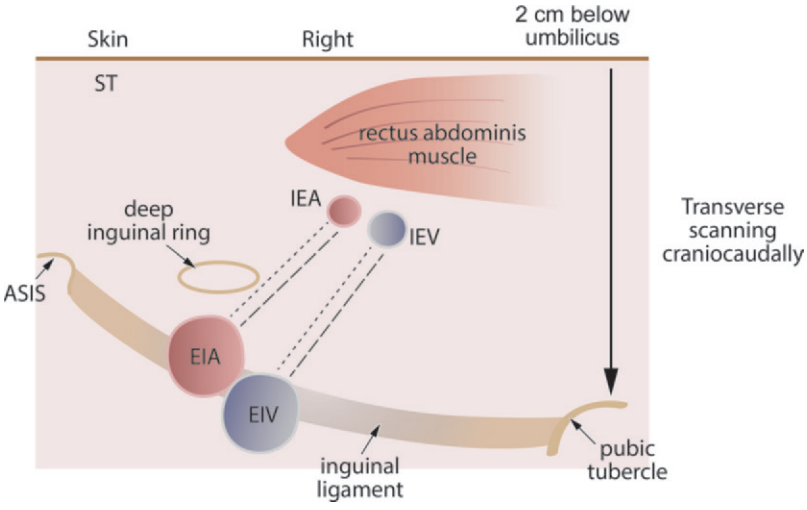

Figure 6. Diagram illustrates the imaging landmarks used for localization of the deep inguinal ring of the IC, as shown on the transverse view through the right side of the abdomen. The deep inguinal ring is lateral to the origins of the inferior epigastric artery *(IEA)* and inferior epigastric vein *(IEV)*. These vessels are posterior to the lateral border of the rectus abdominis muscle, approximately 2 cm below the umbilicus. *ASIS* = anterior superior iliac spine, *EIA* = external iliac artery, *EIV* = external iliac vein, *ST* = soft tissues.

frequency (ie, 3–5-MHz) curved transducers are reserved for examination of larger patients or cases in which additional depth is required for a complete evaluation. The acquisition of comparison views of the contralateral side is advised when symptoms are focal and no definitive US findings are discovered (9).

Identification of the IC at US is based primarily on localization of the deep inguinal ring, which is just lateral and slightly cephalic to the origins of the inferior epigastric vessels, which are best identified by placing the transducer on the short axis relative to the rectus abdominis muscle, about 2 cm inferior to the umbilicus. The transducer is then moved caudally until the inferior epigastric vessels (two veins and one artery) are seen lying just deep to the lateral border of the rectus abdominis muscle (Fig 6). Subsequently, the vessels are tracked inferolaterally to their origin at the external iliac vessels (Movie 1) (10). Once

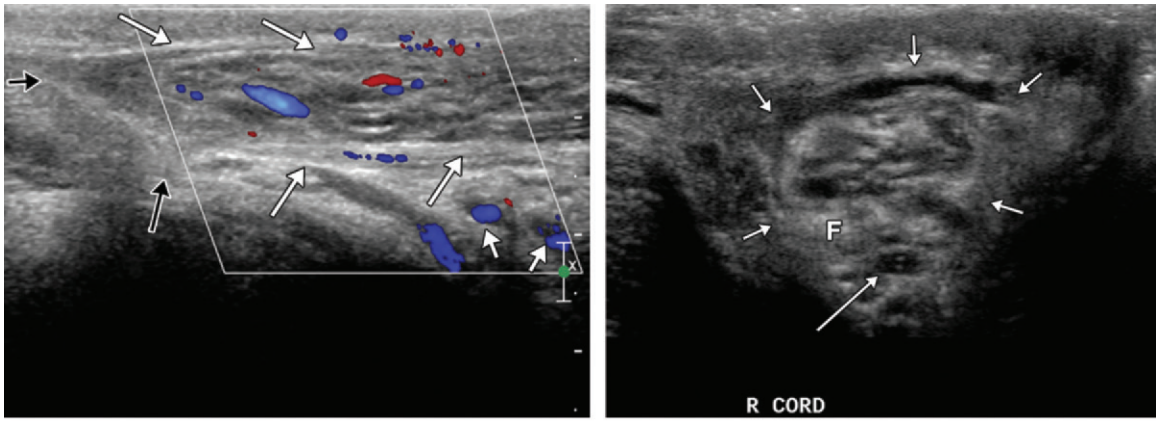

a. b.

Figure 7. US identification of the IC in a 53-year-old man. **(a)** Axial oblique color Doppler US image obtained with the transducer on the long axis relative to the IC with the patient at rest shows the deep inguinal ring as an opening in the peritoneum (black arrows) that allows passage of the spermatic cord and vessels into the IC (long white arrows). The inferior epigastric vessels (short white arrows) are located deep to the IC. **(b)** Sagittal gray-scale US image obtained with the transducer on the short axis relative to the IC while the patient performed the Valsalva maneuver shows a soft-tissue rim (short arrows) outlining the contents of the IC. Note the prominent vascular structures and fat infiltration *(F)* along the cord. The vas deferens (long arrow) also is seen.

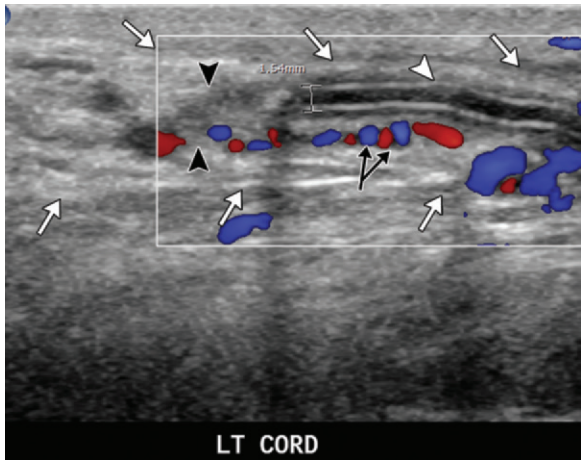

Figure 8. US anatomy of the contents of the spermatic cord in a 46-year-old man. Sagittal color Doppler US image demonstrates the normal vas deferens (white arrowhead) as a hypoechoic tubular structure with linear reflectors in the spermatic cord (black arrowheads). The vas deferens is 1.5 mm in diameter. The testicular vessels (black arrows) are adjacent to the vas deferens. The spermatic cord is slightly more hypoechoic than the rest of the IC contents. The IC is outlined by the white arrows.

the deep inguinal ring is located on the short axis, the transducer can be angled along the expected course of the IC, slightly cranial and parallel to the medial half of the inguinal ligament (Movie 1). The inguinal ligament characteristically appears on US images as an echogenic cord extending between the anterior superior iliac spine and the pubic tubercle, a major bone landmark of the inguinal region (7). Images are acquired in a sagittal oblique plane on the short axis relative to the IC and in an axial oblique plane on the long axis relative to the IC (Fig 7). The contents of the IC should be carefully examined by using both gray-scale and color Doppler US, with the patient performing the Valsalva maneuver and/or standing during the examination, to assess for possible hernias, varicoceles, and other pathologic processes (Movie 1) (7). The normal deep inguinal ring may not be easy to see because it will be collapsed and closed. Small craniocaudal movements of the probe while it is oriented in the axial oblique plane may help in identifying the contents of the cord entering the deep ring, further aiding in identification of this ring.

The normal contents of the IC have a specific US appearance. In male patients, the suprascrotal segment of the vas deferens appears as a cordlike hypoechoic structure with central parallel linear reflectors that represent the walls of the lumen (11). The normal size of the vas deferens is 1–3 mm in anteroposterior diameter. At color Doppler US, the testicular artery and pampiniform plexus are readily visualized as tubular vessels coursing along the IC. The spermatic cord, containing the vas deferens and testicular vessels, is relatively hypoechoic compared with the echogenic fat in the IC (Fig 8). The US appearance of the IC may vary according to the extent of fat infiltration along the cord. Echogenic infiltrating fat is seen along the spermatic cord throughout the course of the IC and is continuous with the peritoneum cranially; this finding helps to differentiate benign fat infiltration from a fat-containing mass such as a lipoma (8).

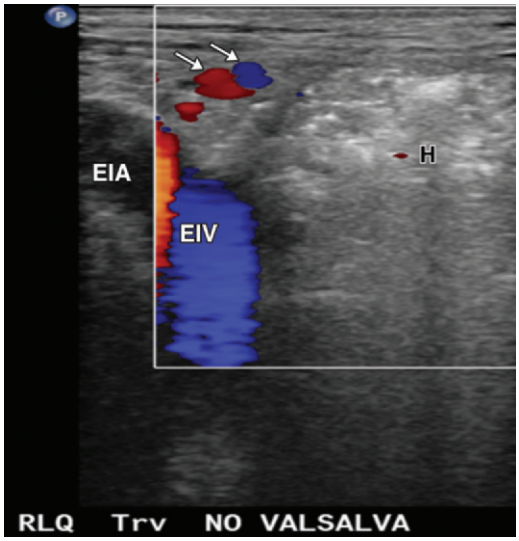

Figure 9. Direct inguinal hernia in a 52-year-old man with groin pain. A large fat- and bowel-containing hernia sac *(H)* is located medial to the inferior epigastric vessels (arrows) in the Hesselbach triangle. *EIA* = external iliac artery, *EIV* = external iliac vein. The hernia sac is not reducible when the patient is at rest.

Hernia

An inguinal hernia is a protrusion of the intra-abdominal structures into the IC. There are two major types of inguinal hernias: the indirect type, which represents 50% of all inguinal hernias, and the direct type, which represents up to 25% of these protrusions (12). Up to 6.8% of patients are found to have combined direct and indirect hernias (13). Although femoral hernias also are considered groin hernias, they do not involve the IC.

An indirect inguinal hernia occurs when abdominal contents protrude through the deep inguinal ring and course anteromedially to the spermatic cord in the IC (Movie 2). The hernia contents emerge by way of the superficial ring and often descend into the scrotum or labia majora (5). Indirect inguinal hernias are more common in men and are considered to be congenital, as 90% of cases are associated with a patent PV (14,15). They occur most commonly on the right side.

Direct hernias are not congenital and tend to occur in older individuals as a result of relaxation of the abdominal wall musculature and thinning of the fascia. They are commonly bilateral. Any condition that results in either increased intra-abdominal pressure or abnormal collagen may cause development of a direct inguinal hernia. Risk factors include chronic obstructive pulmonary disease, heavy lifting, ascites, coughing, peritoneal dialysis, smoking, and collagen-vascular disease. Direct inguinal hernias enter the IC through a defect in the conjoint aponeurosis of the posterior wall of the IC.

US has an essential role in accurate diagnosis and evaluation of inguinal hernias and high accuracy in detection of both clinically suspected and occult hernias; however, it is operator dependent. The type of inguinal hernia can be determined at US by identifying the hernia neck and its relationship to the inferior epigastric vessels, and observing the characteristic movement of the contents of the hernia with respect to the transducer at provocative maneuvering (5). The deep inguinal ring is the neck of an indirect inguinal hernia and is located lateral to the origin of the inferior epigastric vessels (Movie 3). The neck of a direct inguinal hernia lies medial to the inferior epigastric vessels within the Hesselbach triangle (Fig 9). Because direct inguinal hernias can occur anywhere in the Hesselbach triangle, the entire triangle should be interrogated incrementally by using the Valsalva maneuver. Surveillance for possible hernias should be performed throughout the entire maneuver, as augmentation of the hernia sac can be observed during the positive-pressure and relaxation phases of the Valsalva maneuver. The contents of a direct hernia sac will move toward the US transducer. The Valsalva maneuver–induced movement of an indirect inguinal hernia is more complex than that of a direct hernia. At the level of the deep inguinal ring, the indirect hernia contents will move toward the transducer. Once the contents are in the canal, they will move along the axis of the IC anteromedially and inferiorly. When the hernia sac emerges from the superficial ring, the hernia contents will again move toward the transducer. The characteristic movement of the hernia contents might not be detected if the patient is unable to perform the Valsalva maneuver adequately or the hernia contents are incarcerated. Having the patient stand upright or using other provocative maneuvers may help induce herniation. A potential pitfall in detection of hernias is related to the normal movement of the spermatic cord, which when observed during the Valsalva maneuver is considered a sign of an indirect inguinal hernia (Movie 4). A lack of distension of the IC during the Valsalva maneuver while scanning on the short axis relative to the IC should help to avoid this misdiagnosis. Another potential pitfall is misinterpretation of abdominal wall movement as a direct inguinal hernia. The general rule is that at Valsalva maneuvering, the abdominal wall will move as one unit, with no translation of the presumed hernia content separately and anterior to the inferior epigastric vessels (5).

The hernia sac can contain a variety of intra-abdominal structures such as mesenteric fat, the small bowel, the ascending and/or descending colon, the urinary bladder, ovaries, the appendix, and ureters. The contents of the hernia sac may become incarcerated or strangulated. A hernia is considered to be incarcerated or irreducible if the contents cannot return to the abdomen either

Figures 10, 11. **(10)** Spontaneously reducible inguinal hernia in a 3-month-old boy who presented with a lump in the right groin area. **(a)** Sagittal gray-scale US image obtained during the Valsalva maneuver shows a large hernia sac (white arrows) in the IC; the sac contains a loop of small bowel (*). Note the neck (black arrows) of the hernia. **(b)** Transverse gray-scale US image obtained with the patient at rest shows a nearly complete spontaneous reduction of the hernia. Only a small amount of omental fat remains in the residual hernia (arrows). **(11)** Nonreducible, or incarcerated, indirect inguinal hernia containing a loop of bowel in a 5-year-old girl who presented with abdominal pain. Sagittal gray-scale US image demonstrates a loop of fluid-filled bowel (arrows) in the hernia sac (arrowheads). A small amount of surrounding free fluid (*) also is present in the hernia sac. Vascular flow was present in the wall of the herniated bowel, but no peristalsis was noted (not shown).

10a.

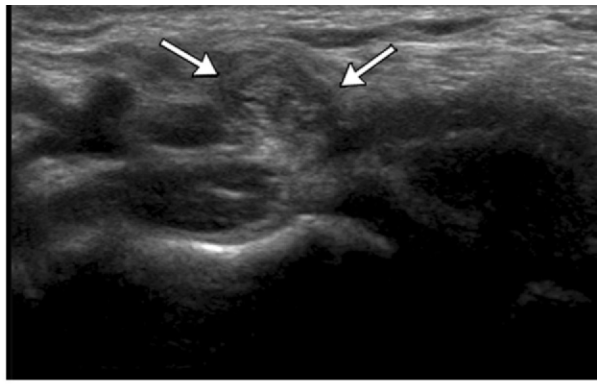

10b.

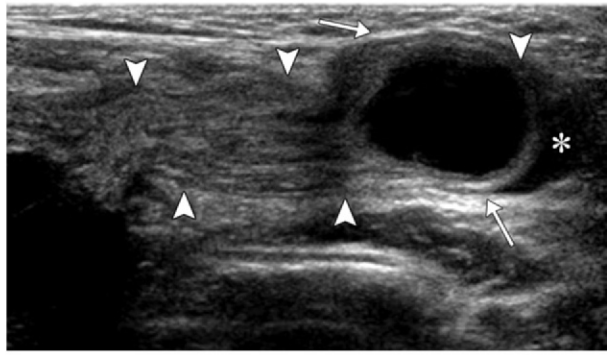

11.

spontaneously or with compression (Figs 10, 11) (Movies 5, 6).

Strangulated hernias are characterized by a compromised blood supply to the hernia contents. Signs of potential ischemia include free fluid in the hernia sac, organ or wall edema, and absence of bowel peristalsis that results in flaccid bowel. Color and power Doppler US examinations are helpful in assessing ischemia of the hernia sac contents. Hyperemia is usually seen during the early stages of strangulation, and the absence of blood flow is usually seen during the late stages. Swirling of mesenteric vessels, or the "whirlpool" sign, can be seen when the contents of the hernia sac abnormally twist on themselves and cause a compromise of the blood supply to the affected structure (7). Air in the hernia sac, peritoneal cavity, or bowel wall (ie, pneumatosis intestinalis) is a sign of bowel necrosis or perforation (16).

An obstructed hernia is a bowel-containing hernia that results in obstruction of the bowel lumen—usually at the hernia neck. Although the loops of bowel in the hernia sac generally are not dilated, the presence of bowel in the sac should prompt the examiner to assess the abdomen for signs of bowel obstruction.

Management of Inguinal Hernias

Inguinal hernias are most commonly repaired with placement of a polypropylene-polytetrafluoroethylene mesh or mesh plug across the deficient tissues that lie between the peritoneum and the transversalis fascia, deep to the IC. At US, a mesh appears as an echogenic structure, with posterior acoustic shadowing that results from the US beam reflection from the surface of the mesh. Deeper anatomic structures usually are obscured by the strong posterior shadowing (Fig 12). Use of an extended field of view may help in identifying mesh on US images. With older repaired hernias, a wavy appearance of the mesh may be seen owing to mesh shrinkage that results from healing and formation of fibrous tissue or a scar (8,17).

Postoperative Complications

Seromas, Hematomas, and Abscesses

Seroma or hematoma formation is a common complication that occurs after laparoscopic or open hernia repair; the incidence of this complication ranges from 5% to 25% (18). Seromas and hematomas are most commonly seen after repair of large indirect hernias or after emergent (as opposed to elective) hernia repair. Most seromas and hematomas resolve within 4–6 weeks. Other common causes of hematomas in the IC include excessive anticoagulation, trauma, and other surgical procedures (19). Patients may present with an enlarging groin mass. At US, hematomas may be seen as simple anechoic fluid collections in the IC or fluid collections with

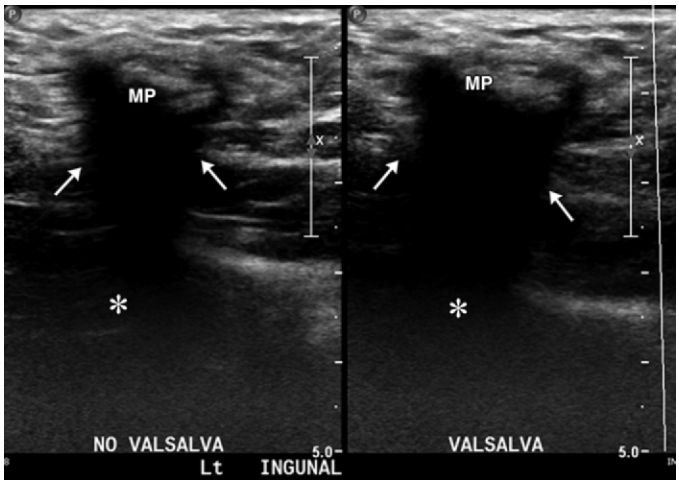

Figure 12. Normal appearance of a mesh plug *(MP)* in a 45-year-old man after hernia repair. Transverse oblique US images obtained with (right) and without (left) Valsalva maneuvering show strong posterior acoustic shadowing (*) from the mesh plug. Note the site of entry of the mesh into the deep inguinal ring (arrows). No change was observed with Valsalva maneuvering; this finding is consistent with an intact mesh plug.

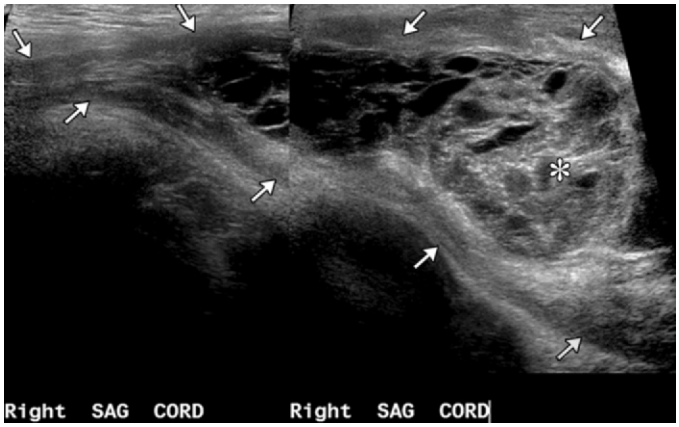

Figure 13. Postoperative hematoma in a 45-year-old man with scrotal swelling and pain 11 days after inguinal hernia repair. Sagittal gray-scale montage US image demonstrates marked distension of the right IC (arrows) caused by a complex heterogeneous fluid collection (*), which extends into the scrotum. The IC is inflamed and has thickened walls.

thin weblike internal septa (Fig 13). A perioperative hematoma or seroma may be difficult to differentiate from a postoperative abscess, which is a rare postoperative complication. An abscess usually develops during the late postoperative period, more than 30 days after the surgery; however, it may develop earlier (20). On US images, an abscess generally appears as a complex fluid collection—often with associated peripheral hyperemia and echogenic foci, with dirty shadowing indicative of air. When differentiation of these entities is difficult at US, the patient's clinical history can often aid in making the correct diagnosis. Contrast material–enhanced CT can be helpful for confirming the diagnosis and better evaluating the extent of an abscess.

Hernia Recurrence

Hernias recur in 0.5%–15.0% of patients, and this recurrence can be caused by a mesh repair failure such as mesh migration or erosion. On US images, a persistent hernia sac is usually seen along the edge of the linear echogenic mesh, and the posterior acoustic shadowing produced by the mesh aids in recognition of this sac (Movie 7). Migrated mesh material may be seen in the sac of the recurrent hernia (Fig 14).

Other Complications

Infertility can result from vas deferens obstruction after bilateral inguinal hernia repair. Testicular ischemia is a rare but serious complication that occurs after hernia repair; it is usually attributable to mesh obliteration of the testicular artery. At US, injury to the vas deferens should be suspected if the spermatic cord is edematous. Heterogeneous enlargement of the testis in conjunction with a high-resistance arterial waveform or absent blood flow suggests the presence of testicular ischemia (21).

Hydrocele

A hydrocele is a serous fluid collection that occurs in the IC, usually as a result of congenital failure of the PV to obliterate. Congenital hydroceles are present in 6% of male infants at delivery but in fewer than 1% of adults, as most hydroceles resolve by 18 months of age. Hydroceles are typically located anterior and medial to the spermatic cord. Patients present with a bulge in the region of the IC. There are two major types of IC hydrocele: communicating and noncommunicating (Fig 15). With a communicating hydrocele, there is communication of fluid between the

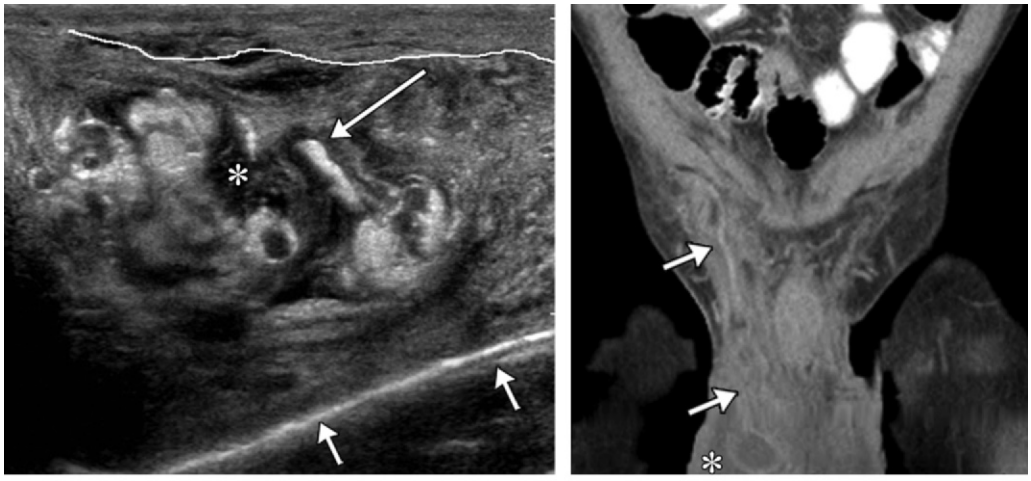

Figure 14. Recurrent inguinal hernia, with a migrated mesh and multiple abdominal and extra-abdominal abscesses, in a 34-year-old man 6 days after hernia repair. **(a)** Sagittal gray-scale US image shows a large right inguinal hernia sac, demarcated by the wavy white line at the top, that contains heterogeneous fluid collections (*), echogenic inflamed fat, loops of small bowel, and echogenic linear material (long arrow) that likely represents the mesh. A linear echogenic area (short arrows), compatible with migration of the mesh, is seen in the hernia. **(b)** Coronal contrast-enhanced CT image of the pelvis shows a crumpled, redundant-appearing plug of mesh (arrows) in the hernia and an associated fluid collection (*). Multiple intra-abdominal abscesses (not shown) also were present.

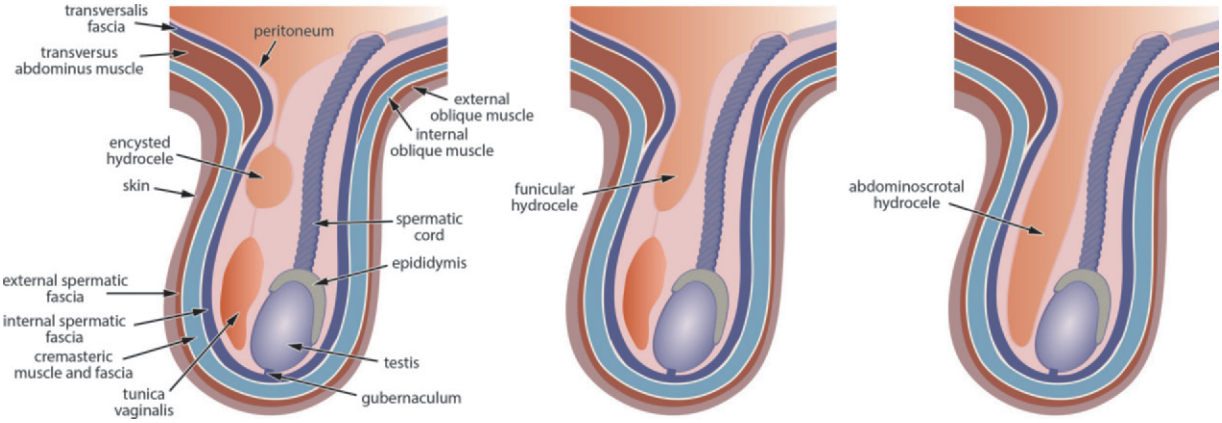

Figure 15. Diagram illustrates the classification of congenital hydroceles. Left: With a noncommunicating encysted hydrocele, fluid is trapped in the remnant of the PV. Middle: With a noncommunicating funicular hydrocele, the fluid collection in the IC communicates with the peritoneal cavity; however, there is no communication with the scrotum. Right: With a communicating (ie, abdominoscrotal) hydrocele, there is communication of fluid between the peritoneal cavity and the scrotum due to complete patency of the PV.

peritoneal cavity and scrotum due to complete patency of the PV (Figs 15, 16). These hydroceles commonly coexist with indirect inguinal hernias. There are two subtypes of noncommunicating hydrocele, also termed *spermatic cord hydrocele:* encysted and funicular. With the encysted subtype, fluid is trapped in the remnant of the PV—or canal of Nuck in female persons—and does not communicate with the peritoneal cavity or scrotum (Figs 15, 17). With the funicular subtype, the fluid collection in the IC communicates with the peritoneal cavity and deep inguinal ring, but it does not communicate with the scrotum (Figs 15, 18). Noncommunicating encysted hydroceles are more common (22–24).

In patients with elevated intra-abdominal pressure—for example, in association with cirrhotic or malignant ascites—the PV may reopen and allow extension of intra-abdominal fluid into the scrotum and, in turn, cause an acquired communicating hydrocele.

On US images, both congenital and acquired hydroceles usually appear as an anechoic fluid collection with no internal vascular flow. Low-level echoes may be seen if debris is present in the fluid. The debris may result from prior infection, hemorrhage, or trauma or be related to proteinaceous material or deposition of cholesterol crystals. Evaluation for possible extension of fluid into the peritoneum and scrotum can

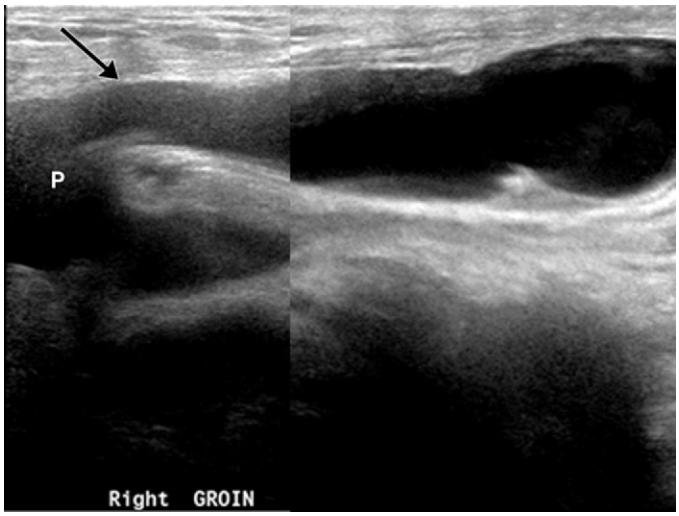

Figure 16. Communicating hydrocele associated with a patent PV in a 59-year-old man with a right scrotal hydrocele and ascites due to cirrhosis. Sagittal gray-scale montage US image demonstrates tracking of the ascites through the IC (arrow), from the peritoneal cavity *(P)* into the scrotum. The scrotal hydrocele and related contents are not shown.

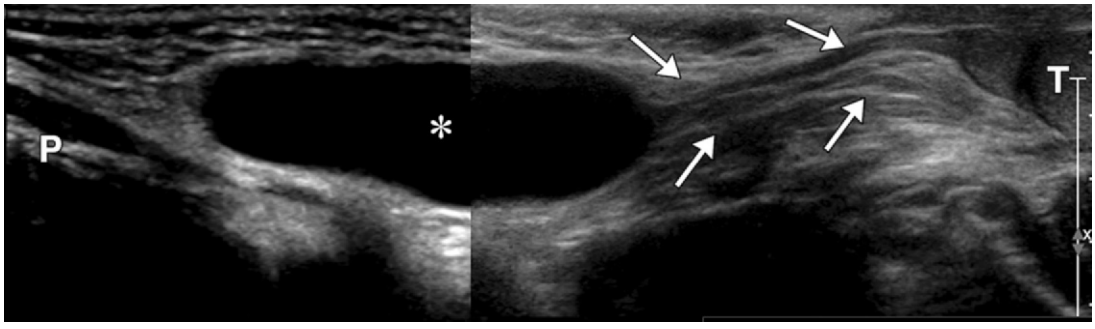

Figure 17. Noncommunicating (spermatic cord) encysted hydrocele in a 10-month-old boy with a palpable right inguinal mass. Sagittal gray-scale montage US image shows an anechoic fluid collection (*) along the spermatic cord in the IC (arrows). The fluid collection is separate from and above the testis *(T)*. No communication with the peritoneal cavity *(P)* is seen. The size of the hydrocele did not change with Valsalva maneuvering (not shown).

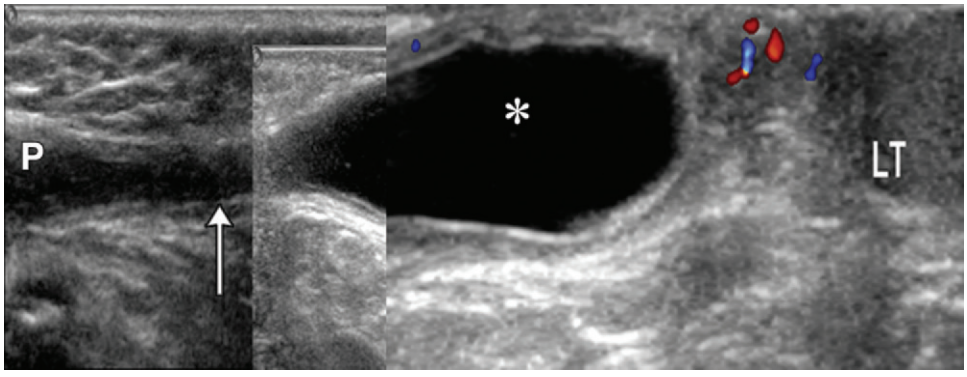

Figure 18. Noncommunicating (spermatic cord) funicular hydrocele in a 3-month-old boy with a palpable right inguinal mass. Sagittal gray-scale and color Doppler montage US image shows an anechoic fluid collection (*) in the IC communicating (arrow) with the peritoneal cavity *(P)*. The fluid does not extend into the scrotum. This spermatic cord hydrocele increased in size with Valsalva maneuvering (not shown). *LT* = left testis.

help determine the correct pathologic variant of hydrocele. The Valsalva maneuver can help differentiate the encysted and funicular variants, with the funicular variant demonstrating a larger size during the maneuver (25). The differential diagnosis includes a large epididymal cyst that extends into the IC (Fig 19).

Varicocele

Varicoceles in Male Individuals

Primary or idiopathic varicoceles are associated with incompetent valves of the pampiniform plexus, which lead to impaired venous drainage and subsequent dilatation of the pampiniform

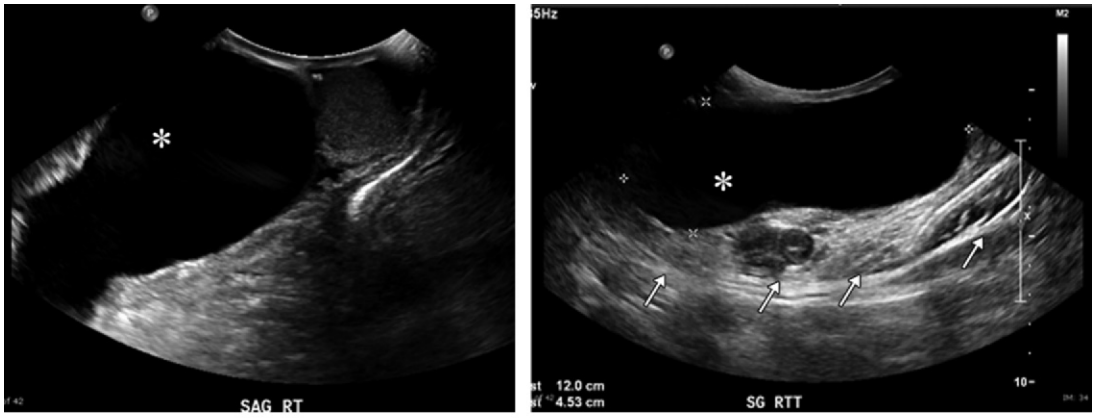

a. b. c.

Figure 19. Epididymal cyst extending into the IC in a 59-year-old man with right testicular pain. **(a, b)** Sagittal US images show a large anechoic, avascular, loculated fluid collection (*) that displaces the testis posteriorly **(a)** and extends into the IC (arrows in **b**) cranially **(b)**. **(c)** Coronal contrast-enhanced CT image shows a fluid-filled structure (*) extending into the right IC. There is no fluid in the peritoneal cavity.

plexus veins. Primary varicoceles are more common on the left side, although bilateral varicoceles may be found in up to 50% of individuals (26). Secondary varicoceles are caused by increased pressure in the testicular vein as a result of intra-abdominal pathologic processes (19,27–29). It is important to note that isolated right-sided varicoceles are seen in only 6% of patients, and if they are detected, the retroperitoneum and abdomen should be evaluated for any pathologic process—most commonly a neoplasm. Varicoceles can also develop as a complication of a prior vasectomy; the reported incidence of such cases is 27% (30). Symptoms include a soft palpable mass in the groin, pain, and/or infertility (31).

On gray-scale US images, varicoceles appear as multiple serpiginous anechoic tubular structures, with a "bag of worms" appearance, along the IC. To establish the diagnosis, the veins of the pampiniform plexus should be greater than 2–3 mm in diameter (2). Conspicuity of the veins increases with the Valsalva maneuver and in the standing position (2,32). Partial or complete thrombosis of a varicocele is common and can be diagnosed when the veins are noncompressible and fill only partially with blood at color Doppler US (Fig 20). Another potential cause of a noncompressible varicocele is a retroperitoneal malignant process (19).

Varicoceles (Round Ligament Varices) in Female Individuals

Varicosities arising from the round ligament are rare, are most commonly seen during pregnancy, and manifest as acute swelling and pain in the groin (33,34). The clinical presentation associated with a round ligament varicocele is similar to that associated with an inguinal hernia, and the distinction between these two entities can be difficult. Gray-scale and color Doppler US examinations aid in this differentiation and thus help to avoid unnecessary surgical intervention. The imaging findings of round ligament varices are the same as those of varicoceles in male persons (Fig 21). Varicosities are usually self-limited and are managed conservatively in pregnant patients since most of them resolve spontaneously after delivery. However, close monitoring is required, as rupture and thrombosis of round ligament varices can occur and result in intense painful swelling in the groin (33,35).

At imaging, thrombosis of a varicocele should be suspected if the veins are noncompressible and no flow signal can be seen. A visible clot may be seen in the lumen. Surgical management is reserved for cases of uncontrollable pain, substantial discomfort from varicocele enlargement, and/or varicocele rupture and thrombosis. Varicoceles can be surgically excised or addressed with embolization. Decompression of the groin may result in alleviation of symptoms (36–38).

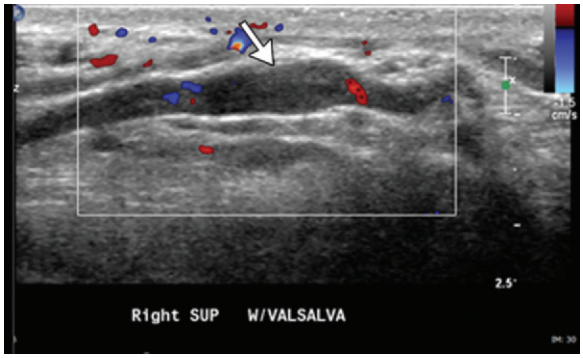

Figure 20. Partially thrombosed IC varicocele in a 21-year-old man after spermatic cord ligation. Sagittal color Doppler US image of the right IC shows a dilated partially thrombosed varicocele (arrow) that contains internal echoes and very little detectable blood flow. An increase in the size of the vein, measuring greater than 3 mm in diameter, was apparent with Valsalva maneuvering.

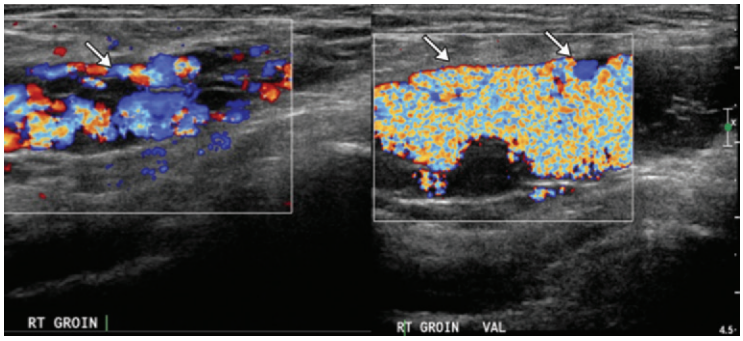

Figure 21. Round ligament varices in a 19-year-old woman who was 8 months pregnant and presented with bilateral groin swelling. Sagittal color Doppler montage US image of the right groin obtained with the patient at rest (left) and after the Valsalva maneuver (right) demonstrates multiple vessels (arrows) in the IC that became more prominent with Valsalva maneuvering. These findings are compatible with varicosities. Similar findings were present on the left side (not shown).

Testicular Ectopia

Undescended Testes

Undescended testes, or cryptorchidism, is a result of developmental arrest of the normal descent of the testes into the scrotum; it occurs in up to 30% of premature infants. The incidence of cryptorchidism, or maldescended testis, in full-term neonates is estimated to be between 2.7% and 5.9% at birth, but it decreases to 1.2% or 1.8% by 1 year of age (39). Spontaneous descent after the 1st year of life is uncommon. Cryptorchidism can be unilateral (90% of cases) or bilateral (10% of cases) (40). Undescended testes may be located in the abdominal cavity or anywhere along the path of their embryologic descent, including retroperitoneal, pelvic, inguinal, and subinguinal locations. Up to 80% of individuals with this condition have testes in the IC (41–43). Undescended testes should not be confused with ectopic testes, a condition in which the testes are located outside of their normal path of descent and found in places such as the superficial inguinal pouch, base of the penis, perineal region, femoral locations, or anterior abdominal wall (43).

Approximately 90% of undescended testes are associated with a patent PV, and in up to 50% of cases, there is a coexisting inguinal hernia (44). In newborns, the risk for torsion of an undescended testis is higher than the risk for torsion of a normally positioned testis. This is attributable to the higher rate of testicular cancer in undescended testes. Testicular cancer may cause twisting of the spermatic cord or a change in the position of the testis. Individuals with an undescended left testicle in situ have an estimated two- to eightfold increase in the risk for developing testicular cancer (45,46). Patients with undescended testes usually are found to have an empty scrotal sac, with or without a groin mass.

Nearly 80% of undescended testes are palpable. US has 45% sensitivity, 78% specificity, and 88% accuracy in the localization of a nonpalpable undescended testis and is more accurate than clinical examination (47,48). At imaging, nonpalpable testes can be localized by using the tracking technique (43). With this technique, the spermatic cord is used as a guide to find the testes. Initially, one can identify the spermatic cord in the IC at the deep inguinal ring by scanning in a sagittal oblique plane on the short axis relative to the IC. Once found, the cord can be "tracked" inferiorly in an attempt to locate the testis along the path of testicular descent. An intra-abdominal location of the testes should be suspected in cases of an inability to find the testes within or distal to the IC (43). Tracking the cord proximal to the IC may help to localize intra-abdominal testes. In cases of intra-abdominal testes, the cord may be looped within the IC.

At gray-scale US, the echogenicity of an undescended testis may vary. Most cryptorchid testes are hypoechoic; however, some of them may

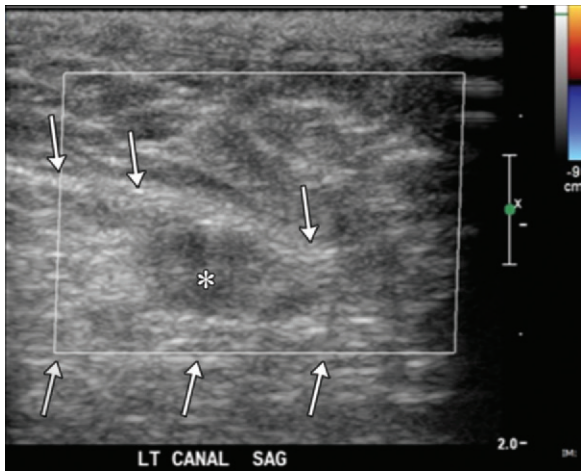

Figure 22. Chronic torsion of a left undescended testis in a 5-year-old boy with an empty left hemiscrotum. Sagittal color Doppler US image of the left IC (arrows) shows an oval hypoechoic, atrophic, undescended testis (*), with no detectable blood flow in the testicular parenchyma. This finding is most compatible with prenatal testicular torsion.

be homogeneously hyperechoic, and coarse or "eggshell" calcifications may be present. Heterogeneity of the testicular parenchyma could be due to the presence of a testicular neoplasm, and in these cases, the parenchyma should be carefully assessed with color and spectral Doppler US. Detection of a testicular mass in an undescended testis may be quite challenging.

In general, undescended testes are relatively small, as compared with normally positioned testes. Testicular atrophy may also be the sequela of a previously unrecognized torsion. Color Doppler US aids in assessment of testicular viability (Fig 22). Concern for possible acute torsion should always be raised when a patient presents with acute groin pain and symptoms indicating an empty scrotum. Although US is the first-line imaging modality for evaluation of testicular torsion, it has decreased accuracy in evaluation of torsion in undescended testes. The main signs of torsion include increased testicle size and absence of detectable blood flow. Torsion should be suspected if venous blood flow is not detected and arterial blood flow has a high resistance pattern; these findings indicate the presence of parenchymal congestion. It is important to note that coexisting hernias may impair visualization of undescended testes, and in these cases, Trendelenburg positioning of the patient or manual decompression of the hernia sac is helpful for improving detection.

In young children, the presence of a testicle in the IC may also be due to a retractile testis. Up to 50% of boys younger than 11 years have at least one retractile testis. The retractile testis can be maneuvered by means of palpation into the scrotal sac, whereas an undescended testis cannot (49). Differentiation of these two entities is very important, as it affects the chosen treatment management.

Patients with cryptorchidism can be treated with hormone therapy, surgery, or a combination of these treatments. Hormone treatment remains controversial, whereas surgery with inguinal orchiopexy is a well-established treatment for a palpable undescended testis (50).

Testicular Dislocation

A testicle in the IC can also result from severe pelvic trauma. Traumatic force can cause the testicles to retract into the IC or be dislocated. Although rare, this occurs as a result of direct external pressure to the perineum that forces the testicle out of the scrotum and into the surrounding tissue. The actual incidence of testicular dislocation is difficult to determine and likely underreported. Bilateral dislocation is rare, constituting only one-third of all cases of testicular dislocation (51). Motorcycle accidents—more specifically, those involving fuel tank injury—are the most commonly reported mechanism (51). Gray-scale US and color Doppler US are the methods of choice for establishing the diagnosis and assessing testicular viability (Fig 23). Once testicular dislocation is detected on one side, the contralateral side also should be evaluated. If the testicle(s) cannot be identified with US, CT can be performed to look for dislocation into the abdominal cavity. Internal dislocation is usually associated with the presence of an inguinal hernia. In cases of delayed diagnoses, persistent dislocation for longer than 1 month has been associated with diffuse atrophy of the seminiferous tubules, nonoccurrence of spermatogenesis, and a theoretical increased risk for neoplastic transformation (52).

Endometriosis

Inguinal endometriosis is a result of ectopic endometrial glands and stroma in the IC. It can be found along the round ligament (53), in inguinal lymph nodes, or embedded in the walls of an inguinal hernia sac (54–59). Surgical excision is

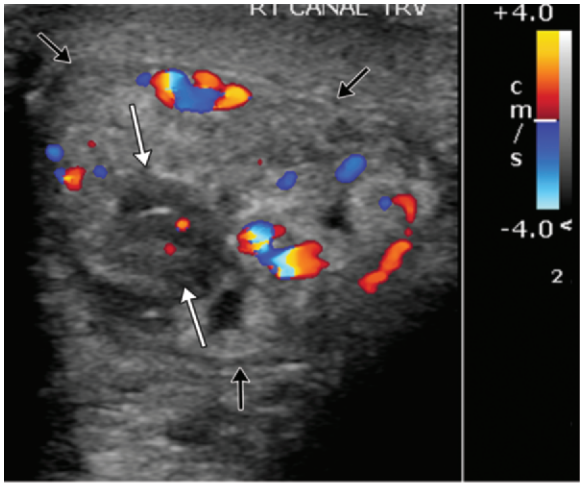

a.

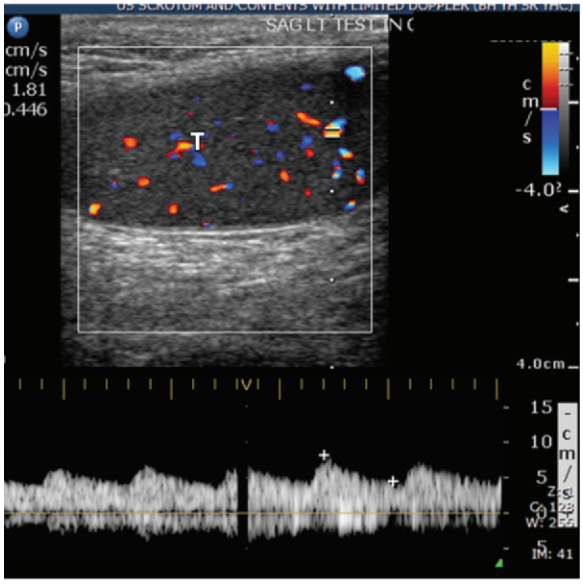

b.

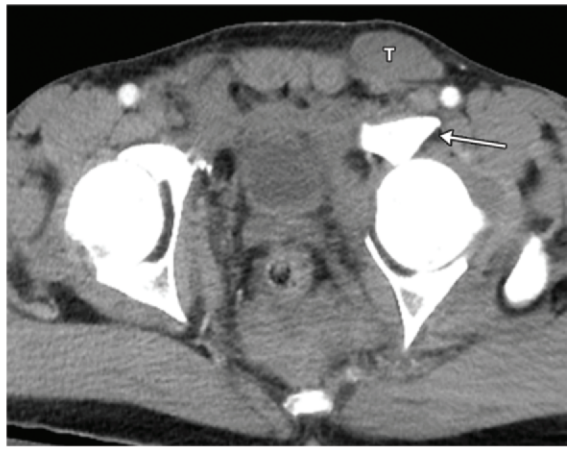

c.

Figure 23. Dislocated testis with spermatic cord injury in a 44-year-old man after a motorcycle collision. **(a)** Transverse color Doppler US image shows an enlarged hypoechoic, heterogeneous, and poorly perfused right spermatic cord (white arrows), with hyperemia of the adjacent structures. The IC (black arrows) is mildly enlarged. **(b)** Sagittal spectral Doppler US image shows the contralateral testis *(T)* dislocated into the IC. Normal low-resistance waveforms, indicating normal perfusion, are present in the dislocated testis. **(c)** Axial contrast-enhanced pelvic CT image shows left acetabular fractures and a left testis *(T)* dislocated into the IC. A comminuted left acetabular fracture (arrow) is seen.

the treatment of choice, as these masses can, on rare occasion, transform into malignancies (59). Ninety-one percent of cases are associated with coexisting pelvic endometriosis (59). The clinical symptoms of inguinal endometriosis may be nonspecific (60). Patients present with a painful lump in the groin and cyclical premenstrual tenderness and/or swelling. A lobulated or irregularly shaped hypoechoic mass with or without blood flow may be seen at US. The presence of blood flow depends on whether the lesion is in an active or dormant state (Fig 24). Cystic changes also may be seen in the mass. US findings are nonspecific, and they may mimic those of a tumor. The imaging appearance of endometriosis varies according to the amount of hemorrhagic change and the degree of fibrosis. Hemosiderin deposition in the lesion at MR imaging is a standard finding of this condition. Characteristic MR imaging findings are high signal intensity on fat-suppressed T1-weighted images and low signal intensity on T2-weighted images (61). The patient's clinical history may help to confirm the diagnosis.

Corditis

The spermatic cord is the main occupant of the IC. When it is inflamed or infected, an associated painful inguinal mass develops. Corditis, also known as vasitis, refers to inflammation of the spermatic cord. Funiculitis refers to inflammation of the suprascrotal portions of the vas deferens. Corditis usually results from the retrograde spread of pathogens from the prostatic urethra, prostate gland, or seminal vesicles (62). The most common pathogens are *Escherichia coli* and *Haemophilus influenzae* (63). US findings include increased size of the spermatic cord, stranding, a heterogeneous appearance of the vas deferens, a masslike appearance of the echogenic fat, a distended IC, and hyperemia that does not change

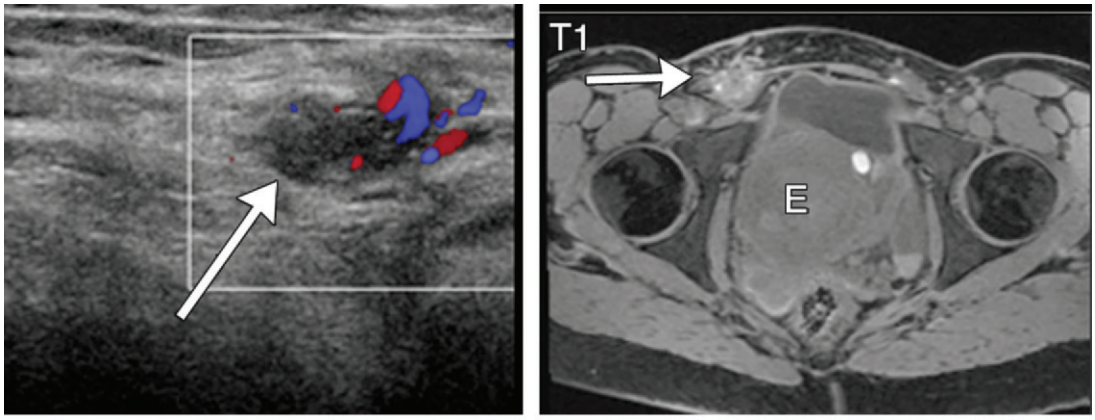

a. b.

Figure 24. IC endometriosis in a 26-year-old woman with cyclic enlargement of and pain in the right groin area. **(a)** Sagittal color Doppler US image shows a poorly defined hypoechoic lesion (arrow) in the IC. This lesion has internal vascularity. The abnormal area corresponds to the area of pain. **(b)** Axial T1-weighted MR image shows intermediate to high signal intensity in the inguinal lesion (arrow). Note the associated large pelvic endometrioma *(E)*.

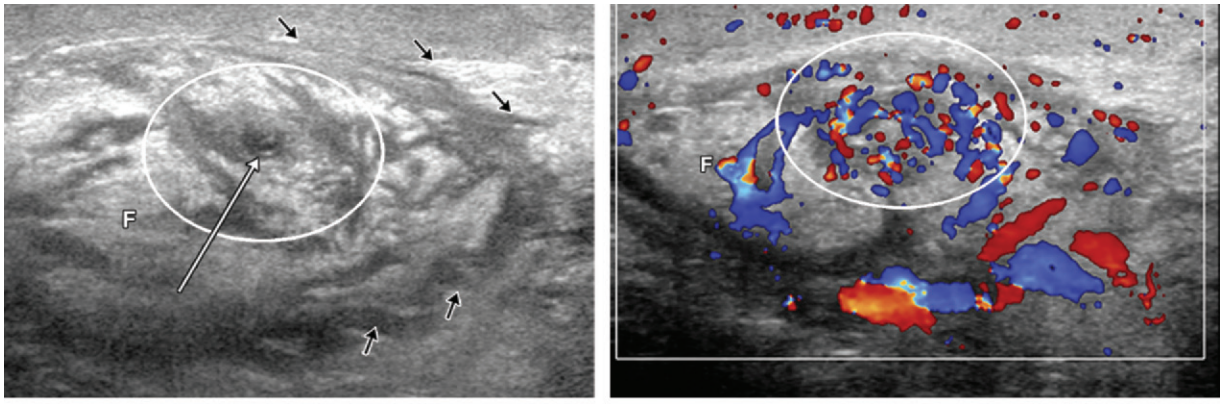

a. b.

Figure 25. Corditis in a 44-year-old man with a history of type I diabetes mellitus and inguinal pain. Transverse gray-scale **(a)** and color Doppler **(b)** US images show a markedly edematous and hyperemic spermatic cord (oval outline) with a central enlarged vas deferens (white arrow in **a**). Note the increased echogenicity of the perispermatic fat *(F),* which is consistent with inflammation. Edema is noted in the surrounding soft tissues (black arrows in **a**).

at Valsalva maneuvering (Fig 25) (11). Dilated vessels and the vas deferens may resemble varicoceles on gray-scale US images. However, dynamic US during the Valsalva maneuver and color Doppler US can aid in differentiating these two entities. Variable degrees of inflammation may be seen, depending on the severity of the process (Fig 26). Severe corditis may have a masslike appearance and result in vascular compromise due to compression of adjacent vessels. This can lead to testicular infarction. Patients are treated with antibiotic agents, although surgical drainage may be required for severe cases (62).

Torsion of the Spermatic Cord

Torsion of the spermatic cord is relatively rare, with the cord twisting occurring most commonly just distal to the superficial inguinal ring. Given the proximity of the spermatic cord twisting to the IC and the associated passive congestion of the venous structures of the more proximal aspect of the spermatic cord, patients often present with inguinal pain and swelling. Use of an extended field of view and/or imaging beyond the IC more distally can facilitate diagnosis of torsion of the spermatic cord (Movie 8).

Neoplasms

Primary neoplasms can arise from any structures of the IC, such as connective tissue, nerve sheaths, muscle, fat, blood vessels, and lymphoid tissue. Benign neoplasms include entities such as lipoma (Fig 27), leiomyoma (Fig 28), lymphangioma (Fig 29), and cystadenoma. Malignant entities include sarcoma, leiomyosarcoma, liposarcoma (Fig 30), rhabdosarcoma, and lymphoma. US findings of malignant neoplasms are nonspecific and often overlap with their benign counterparts. Detailed descriptions of these neoplasms can be found in related articles (32,64,65).

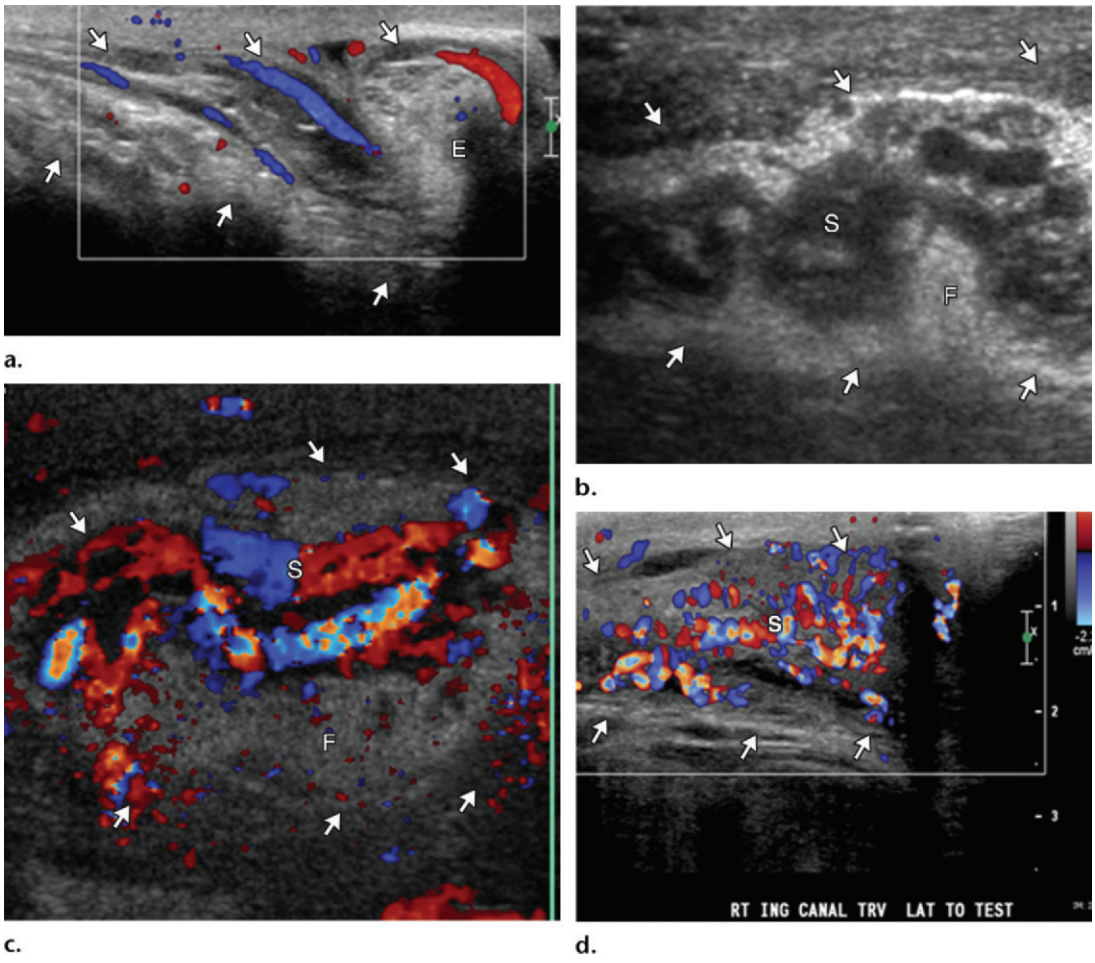

Figure 26. Variable degrees of inflammation of the spermatic cord in three male patients who presented with groin and scrotal tenderness and swelling. **(a)** Sagittal color Doppler US image in a 13-year-old boy shows mild hyperemia of the spermatic cord. The epididymis *(E)* is enlarged and hyperemic. The arrows outline the IC. **(b, c)** Sagittal gray-scale (**b**) and color Doppler (**c**) US images in a 62-year-old man show a moderate degree of spermatic cord *(S)* inflammation. Note the enlarged and hyperemic spermatic cord, inflamed fat *(F)* in the IC, and mildly distended IC (arrows). **(d)** Sagittal color Doppler US image in a 30-year-old man shows severe inflammation of the spermatic cord *(S)* and distension of the IC (arrows).

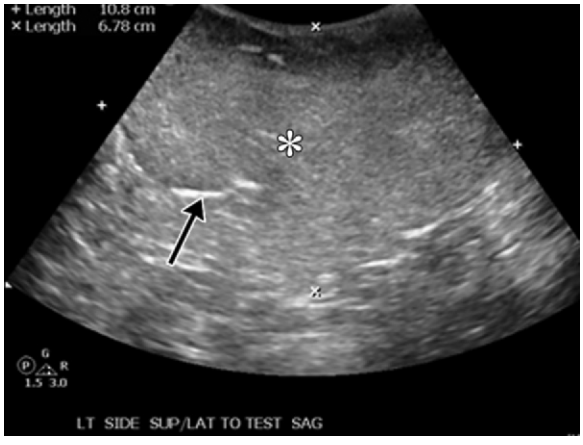

Figure 27. Lipoma of the IC in a 50-year-old man who presented with left testicular swelling. Sagittal gray-scale US image shows distension of the left IC, which contains a large well-circumscribed echogenic avascular mass (*) with linear echogenicities (black arrow) that represent interfaces of fibrous septa. No connection of the lipoma to the retroperitoneal fat was observed at real-time US.

Metastatic Lymphadenopathy

The IC is a common pathway for the metastasis of remote malignant neoplasms, which can occur hematogenously, by way of lymphatic drainage, or by way of local invasion from the adjacent structures—especially bone. The lymphatic drainage system in the inguinal region comprises the superficial and deep inguinal lymph nodes (Fig 31). The superficial lymph nodes, comprising approximately 10 nodes, lie immediately below the inguinal ligament and receive lymphatic drainage from the penis, scrotum, perineum, buttocks, vulva, anus, and abdominal wall below the umbilicus, and

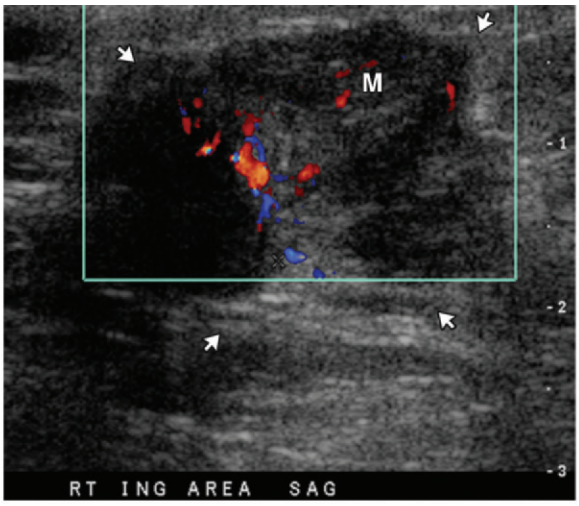

28.

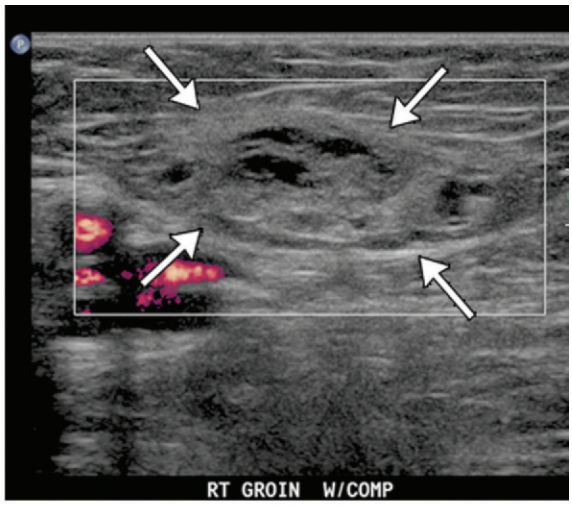

29a.

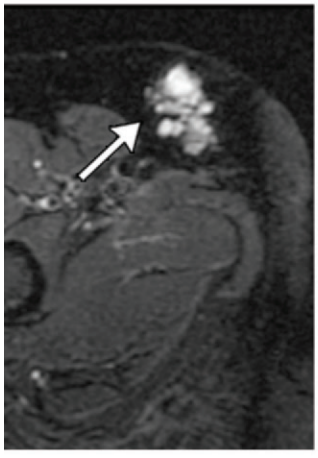

29b.

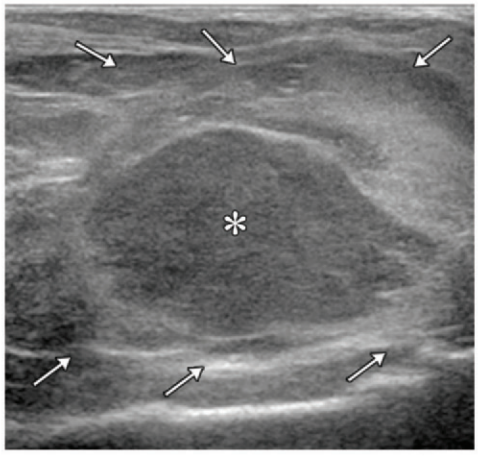

30a.

30b.

Figures 28–30. **(28)** Leiomyoma of the IC in an 18-year-old woman who presented with an enlarging left groin mass. Sagittal color Doppler US image shows a lobulated hypoechoic mass *(M)* with increased vascularity in the IC (arrows). Biopsy revealed an atypical leiomyoma. **(29)** Lymphangioma in a 59-year-old woman who presented with a lump in the right groin area. **(a)** Sagittal color Doppler US image shows a complex heterogeneous cystic mass (arrows) with multiple septa in the right IC. There is no detectable vascular flow. **(b)** Correlative axial T2-weighted fat-suppressed MR image shows a multiloculated cystic lesion (arrow) in the IC. A subtraction MR image enhanced with gadolinium-based contrast material (not shown) showed faint enhancement of the internal septa. **(30)** Liposarcoma of the IC in a 66-year-old man who presented with an enlarging scrotal mass. **(a)** Sagittal gray-scale US image shows a predominantly echogenic heterogeneous avascular mass (*) that has solid components and is distending the right IC (arrows). The mass extended from the scrotum and displaced the right testis laterally and superiorly (not shown). **(b)** Corresponding coronal contrast-enhanced CT image shows a poorly defined fatty mass *(M)* extending into the right IC and displacing the right testis *(T)* superiorly.

these nodes drain into the deep inguinal lymph nodes. The deep inguinal lymph nodes are medial to the femoral vein and comprise about three to five lymph nodes. They drain superiorly to the external iliac lymph nodes, then to the pelvic lymph nodes, and on to the paraaortic lymph nodes (66).

At US, metastatic lymph nodes usually are enlarged, round or have irregular borders, and heterogeneous or hypoechoic, with variable vascular flow. A normal echogenic hilum usually is not apparent. Cystic changes and tiny foci of echogenicity corresponding to calcifications should always raise suspicion for pathologic lymph nodes (Figs 32, 33). When inguinal lymph node metastases are suspected, US-guided biopsy can be performed (67,68).

Metastatic lymphadenopathy should be differentiated from reactive lymphadenopathy, which can result from an infectious or inflammatory process. Enlarged but benign-appearing lymph nodes with echogenic hila are typical US features of reactive lymph nodes (Fig 34). Common benign causes of lymphadenopathy include viral infection (in children), cellulitis, and certain medications. In immunocompromised patients such as those with acquired immunodeficiency syndrome, the differential diagnosis may also include activated tuberculosis, cryptococcosis, cytomegalovirus infection, and toxoplasmosis.

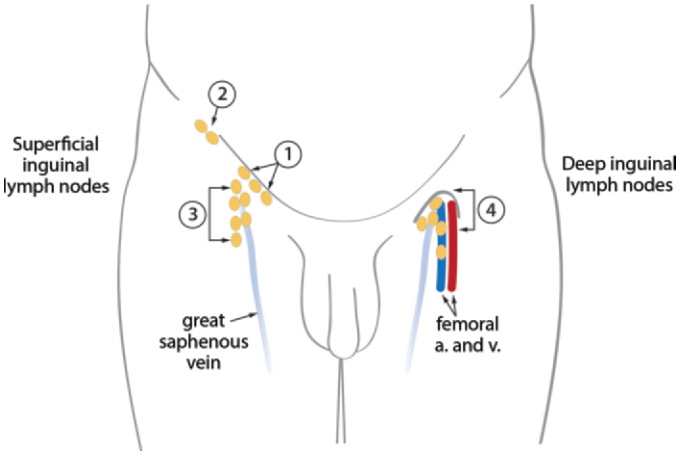

Figure 31. Diagram of lymph nodes of the inguinal region. The superficial inguinal lymph nodes can be divided into three groups: superomedial *(1),* superolateral *(2),* and inferior inguinal *(3).* The deep inguinal lymph nodes *(4)* are located at the femoral ring, just medial to the femoral vein, below the junction with the great saphenous vein. *a.* = artery, *v.* = vein.

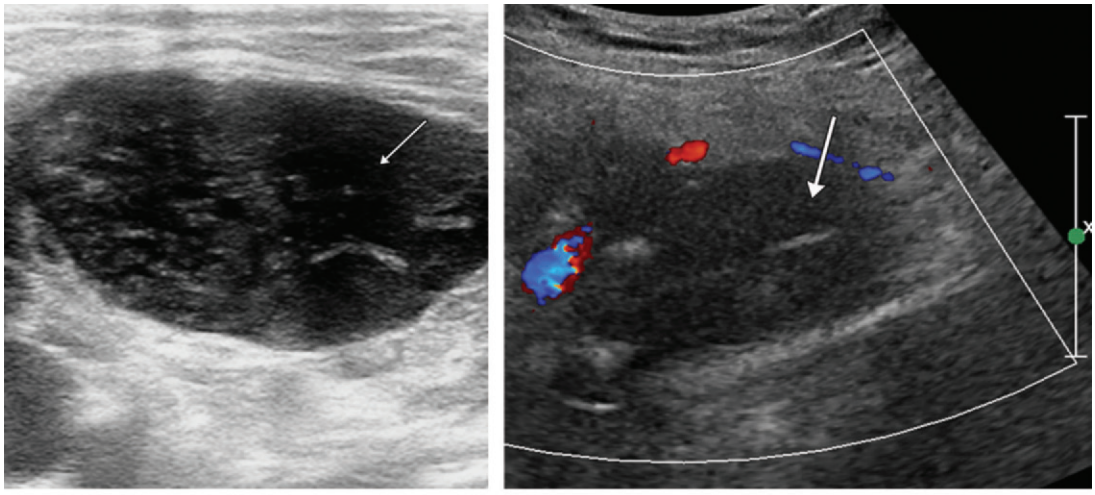

Figure 32. IC metastases from penile cancer in a 50-year-old man. **(a, b)** Sagittal gray-scale **(a)** and color Doppler **(b)** US images show enlarged diffusely hypoechoic inguinal lymph nodes (arrow) with cystic components and without normal fatty hila. Minimal irregular vascularity is present. **(c)** Coronal positron emission tomographic (PET)/CT image shows increased radiotracer uptake (arrows) in the bilateral inguinal regions and distal aspect of the penis.

Conclusion

Many pathologic conditions can affect the IC. To accurately interpret findings and establish the correct diagnosis, it is essential to have a thorough knowledge of the regional US-depicted anatomy, optimal US scanning techniques, and US features of various benign and malignant pathologic conditions that can occur in the IC. Correlative imaging modalities such as CT and MR imaging have a complementary role in evaluation of the IC and aid in assessment of disease extent.

Acknowledgments.—The authors thank Henry Douglas for preparation of the images, Mark Saba for assistance with the illustrations, Lei Wang for helping with video recording, Denise Hersey for assistance with the literature, and Sasha Avinger for obtaining the US images.

Disclosures of Conflicts of Interest.—**L.M.S.** *Activities related to the present article:* disclosed no relevant relationships. *Activities not related to the present article:* educational consultant for Koninklijke Philips. *Other activities:* disclosed no relevant relationships.

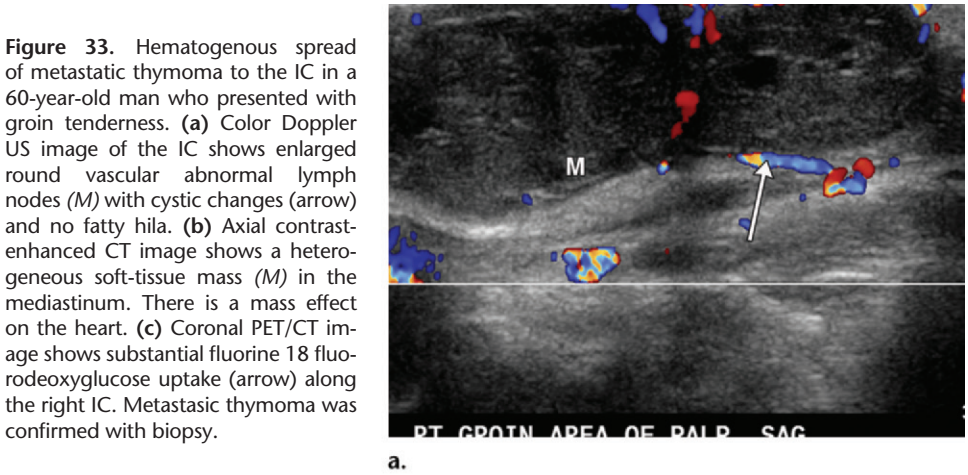

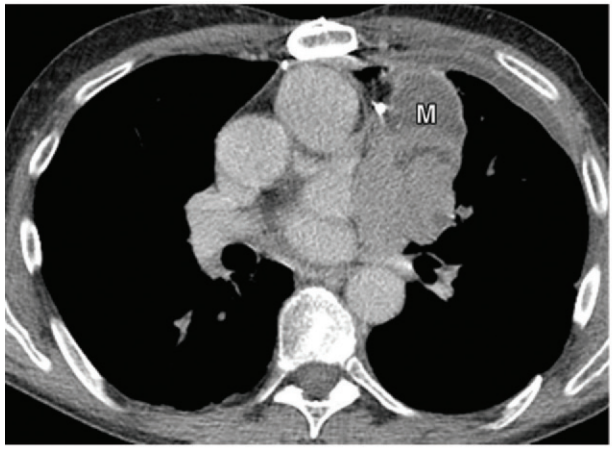

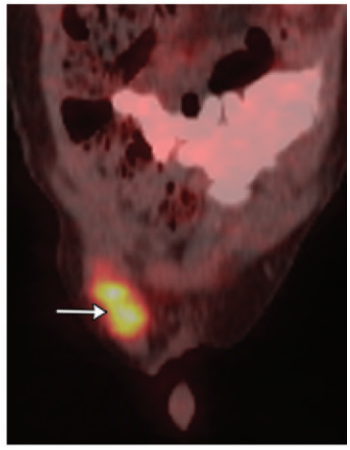

Figure 33. Hematogenous spread of metastatic thymoma to the IC in a 60-year-old man who presented with groin tenderness. **(a)** Color Doppler US image of the IC shows enlarged round vascular abnormal lymph nodes *(M)* with cystic changes (arrow) and no fatty hila. **(b)** Axial contrast-enhanced CT image shows a heterogeneous soft-tissue mass *(M)* in the mediastinum. There is a mass effect on the heart. **(c)** Coronal PET/CT image shows substantial fluorine 18 fluorodeoxyglucose uptake (arrow) along the right IC. Metastasic thymoma was confirmed with biopsy.

Figure 34. Reactive lymph node in a 51-year-old man with lower extremity cellulitis. Transverse gray-scale US image of the left groin area shows an enlarged and elongated benign-appearing lymph node with a characteristic echogenic hilum *(H)*.

References

1. Merchant-Larios H, Moreno-Mendoza N. Onset of sex differentiation: dialog between genes and cells. Arch Med Res 2001;32(6):553–558.
2. Shadbolt CL, Heinze SB, Dietrich RB. Imaging of groin masses: inguinal anatomy and pathologic conditions revisited. RadioGraphics 2001;21(Spec No):S261–S271.
3. Moore KL, Persaud TVN. Urogenital system. In: Moore KL, Persaud TVN, eds. The developing human: clinically oriented embryology. 5th ed. Philadelphia, Pa: Saunders, 1993; 93.
4. Moore KL, Persaud TVN. The urogenital system. In: Moore KL, Persaud TVN, eds. The developing human: clinically oriented embryology. 6th ed. Philadelphia, Pa: Saunders, 1998; 303–348.
5. Jamadar DA, Jacobson JA, Morag Y, et al. Sonography of inguinal region hernias. AJR Am J Roentgenol 2006;187(1):185–190.
6. Moore KL, Dalley AF. Abdomen. In: Moore KL, Dalley AF, eds. Clinically oriented anatomy. 4th ed. Philadelphia, Pa: Lippincott Williams & Wilkins, 1999; 175–330.
7. Burlison JS, Williamson MR. Ultrasonography of hernias. Ultrasound Clin 2014;9(3):471–487.
8. Jamadar DA, Franz MG. Inguinal region hernias. Ultrasound Clin 2007;2(4):711–725.
9. Wagner JM, North JC. Ultrasound of the abdominal wall. Ultrasound Clin 2014;9(4):775–791.
10. Yoong P, Duffy S, Marshall TJ. The inguinal and femoral canals: a practical step-by-step approach to accurate sonographic assessment. Indian J Radiol Imaging 2013;23(4):391–395.
11. Middleton WD, Dahiya N, Naughton CK, Teefey SA, Siegel CA. High-resolution sonography of the normal extrapelvic vas deferens. J Ultrasound Med 2009;28(7):839–846.
12. Katz DA. Evaluation and management of inguinal and umbilical hernias. Pediatr Ann 2001;30(12):729–735.
13. Gurer A, Ozdogan M, Ozlem N, Yildirim A, Kulacoglu H, Aydin R. Uncommon content in groin hernia sac. Hernia 2006;10(2):152–155.

14. Stavros AT, Rapp C. Dynamic ultrasound of hernias of the groin and anterior abdominal wall. Ultrasound Q 2010;26(3):135–169.
15. He D, Lin T, Wei G, et al. Laparoscopic orchiopexy for treating inguinal canalicular palpable undescended testis. J Endourol 2008;22 (8):1745–1749.
16. Rettenbacher T, Hollerweger A, Macheiner P, et al. Abdominal wall hernias: cross-sectional imaging signs of incarceration determined with sonography. AJR Am J Roentgenol 2001;177(5):1061–1066.
17. Jamadar DA, Jacobson JA, Girish G, et al. Abdominal wall hernia mesh repair: sonography of mesh and common complications. J Ultrasound Med 2008;27(6):907–917.
18. Matthews RD, Anthony T, Kim LT, et al. Factors associated with postoperative complications and hernia recurrence for patients undergoing inguinal hernia repair: a report from the VA Cooperative Hernia Study Group. Am J Surg 2007;194(5):611–617.
19. Dogra VS, Gottlieb RH, Oka M, Rubens DJ. Sonography of the scrotum. Radiology 2003;227(1):18–36.
20. Bernardotto M, Jenkinson A. Outcomes in patients who underwent both laparoscopic and open inguinal hernia repairs. ANZ J Surg 2010; 80(5):381–382.
21. Groin hernia: Inguinal and femoral repair. American College of Surgeons: Division of Education. https://www.facs.org/~/media/files /education/patient%20ed/hernrep.ashx. Published May 2013. Accessed May 27, 2015.
22. Kingsnorth AN, Skandalakis PN, Colborn GL, Weidman TA, Skandalakis LJ, Skandalakis JE. Embryology, anatomy, and surgical applications of the preperitoneal space. Surg Clin North Am 2000;80 (1):1–24.
23. Chang YT, Lee JY, Wang JY, Chiou CS, Chang CC. Hydrocele of the spermatic cord in infants and children: its particular characteristics. Urology 2010;76(1):82–86.
24. Martin LC, Share JC, Peters C, Atala A. Hydrocele of the spermatic cord: embryology and ultrasonographic appearance. Pediatr Radiol 1996;26(8):528–530.
25. Garriga V, Serrano A, Marin A, Medrano S, Roson N, Pruna X. US of the tunica vaginalis testis: anatomic relationships and pathologic conditions. RadioGraphics 2009;29(7):2017–2032.
26. Doherty FJ. Ultrasound of the nonacute scrotum. Semin Ultrasound CT MR 1991;12(2):131–156.
27. Keoghane SR, Jones L, Wright MP, Kabala J. Percutaneous retrograde varicocele embolisation using tungsten embolisation coils: a five year audit. Int Urol Nephrol 2001;33(3):517–520.
28. Schulte-Baukloh H, Kämmer J, Felfe R, Stürzebecher B, Knispel HH. Surgery is inadvisable: massive varicocele due to portal hypertension. Int J Urol 2005;12(9):852–854.
29. Ting AC, Cheng SW. Nutcracker phenomenon presenting as left varicocele. Hong Kong Med J 2002;8(5):380.
30. Reddy NM, Gerscovich EO, Jain KA, Le-Petross HT, Brock JM. Vasectomy-related changes on sonographic examination of the scrotum. J Clin Ultrasound 2004;32(8):394–398.
31. Agarwal A, Prabakaran S, Allamaneni SS. Relationship between oxidative stress, varicocele and infertility: a meta-analysis. Reprod Biomed Online 2006;12(5):630–633.
32. Woodward PJ, Schwab CM, Sesterhenn IA. From the archives of the AFIP: extratesticular scrotal masses—radiologic-pathologic correlation. RadioGraphics 2003;23(1):215–240.
33. Chi C, Taylor A, Munjuluri N, Abdul-Kadir R. A diagnostic dilemma: round ligament varicosities in pregnancy. Acta Obstet Gynecol Scand 2005;84(11):1126–1127.
34. Tomkinson JS, Winterton WR. Varicoceles of the round ligament in pregnancy, simulating inguinal herniae. BMJ 1955;1(4918): 889–890.
35. al-Qudah MS. Postpartum pain due to thrombosed varicose veins of the round ligament of the uterus. Postgrad Med J 1993;69(816): 820–821.
36. Cheng D, Lam H, Lam C. Round ligament varices in pregnancy mimicking inguinal hernia: an ultrasound diagnosis. Ultrasound Obstet Gynecol 1997;9(3):198–199.
37. Uzun M, Akkan K, Coşkun B. Round ligament varicosities mimicking inguinal hernias in pregnancy: importance of color Doppler sonography. Diagn Interv Radiol 2010;16(2):150–152.
38. McKenna DA, Carter JT, Poder L, et al. Round ligament varices: sonographic appearance in pregnancy. Ultrasound Obstet Gynecol 2008;31(3):355–357.
39. Pillai SB, Besner GE. Pediatric testicular problems. Pediatr Clin North Am 1998;45(4):813–830.
40. Stone KT, Kass EJ, Cacciarelli AA, Gibson DP. Management of suspected antenatal torsion: what is the best strategy? J Urol 1995;153 (3 Pt 1):782–784.
41. MacKinnon AE. The undescended testis. Indian J Pediatr 2005;72 (5):429–432.
42. Elder JS. The undescended testis: hormonal and surgical management. Surg Clin North Am 1988;68(5):983–1005.
43. Vijayaraghavan SB. Sonographic localization of nonpalpable testis: tracking the cord technique. Indian J Radiol Imaging 2011;21(2): 134–141.
44. Pescovitz OH, Eugster EA. Pediatric endocrinology: mechanisms, manifestations, and management. Philadelphia, Pa: Lippincott Williams & Wilkins, 2004.
45. Pettersson A, Richiardi L, Nordenskjold A, Kaijser M, Akre O. Age at surgery for undescended testis and risk of testicular cancer. N Engl J Med 2007;356(18):1835–1841.
46. Dieckmann KP, Pichlmeier U. Clinical epidemiology of testicular germ cell tumors. World J Urol 2004;22(1):2–14.
47. Tasian GE, Copp HL, Baskin LS. Diagnostic imaging in cryptorchidism: utility, indications, and effectiveness. J Pediatr Surg 2011;46(12): 2406–2413.
48. Adesanya OA, Ademuyiwa AO, Evbuomwan O, Adeyomoye AA, Bode CO. Preoperative localization of undescended testes in children: comparison of clinical examination and ultrasonography. J Pediatr Urol 2014;10(2):237–240.
49. Keys C, Heloury Y. Retractile testes: a review of the current literature. J Pediatr Urol 2012;8(1):2–6.
50. Abacı A, Çatlı G, Anık A, Böber E. Epidemiology, classification and management of undescended testes: does medication have value in its treatment? J Clin Res Pediatr Endocrinol 2013;5(2):65–72.
51. Bromberg W, Wong C, Kurek S, Salim A. Traumatic bilateral testicular dislocation. J Trauma 2003;54(5):1009–1011.
52. Madden JF. Closed reduction of a traumatically dislocated testicle. Acad Emerg Med 1994;1(3):272–275.
53. Jenkins S, Olive DL, Haney AF. Endometriosis: pathogenetic implications of the anatomic distribution. Obstet Gynecol 1986;67(3): 335–338.
54. Majeski J, Craggie J. Scar endometriosis developing after an umbilical hernia repair with mesh. South Med J 2004;97(5):532–534.
55. Pérez-Seoane C, Vargas J, de Agustín P. Endometriosis in an inguinal crural hernia: diagnosis by fine needle aspiration biopsy. Acta Cytol 1991;35(3):350–352.
56. Quagliarello J, Coppa G, Bigelow B. Isolated endometriosis in an inguinal hernia. Am J Obstet Gynecol 1985;152(6 Pt 1):688–689.
57. Brzezinski A, Durst AL. Endometriosis presenting as an inguinal hernia. Am J Obstet Gynecol 1983;146(8):982–983.
58. Goh JT, Flynn V. Inguinal endometriosis. Aust N Z J Obstet Gynaecol 1994;34(1):121.
59. Candiani GB, Vercellini P, Fedele L, Vendola N, Carinelli S, Scaglione V. Inguinal endometriosis: pathogenetic and clinical implications. Obstet Gynecol 1991;78(2):191–194.
60. Majeski J. Scar endometriosis manifested as a recurrent inguinal hernia. South Med J 2001;94(2):247–249.
61. Yang DM, Kim HC, Ryu JK, Lim JW, Kim GY. Sonographic findings of inguinal endometriosis. J Ultrasound Med 2010;29(1): 105–110.
62. Yang DM, Kim HC, Lee HL, Lim JW, Kim GY. Sonographic findings of acute vasitis. J Ultrasound Med 2010;29(12):1711–1715.
63. Chan PT, Schlegel PN. Inflammatory conditions of the male excurrent ductal system. I. J Androl 2002;23(4):453–460.
64. Akbar SA, Sayyed TA, Jafri SZ, Hasteh F, Neill JS. Multimodality imaging of paratesticular neoplasms and their rare mimics. RadioGraphics 2003;23(6):1461–1476.
65. Bhosale PR, Patnana M, Viswanathan C, Szklaruk J. The inguinal canal: anatomy and imaging features of common and uncommon masses. RadioGraphics 2008;28(3):819–835; quiz 913.
66. Bontumasi N, Jacobson JA, Caoili E, Brandon C, Kim SM, Jamadar D. Inguinal lymph nodes: size, number, and other characteristics in asymptomatic patients by CT. Surg Radiol Anat 2014;36(10): 1051–1055.
67. Esen G. Ultrasound of superficial lymph nodes. Eur J Radiol 2006;58 (3):345–359.
68. Stramare R, Beltrame V, Del Villano R, Motta R, Frigo AC, Rubaltelli L. Analysis by high resolution ultrasound of superficial lymph nodes: anatomical, morphological and structural variations. Clin Imaging 2014;38(2):96–99.